

1 Fan, J., Zhang, B., Niu, Y., Luo, A.. and Hao, Y., 2023, Resolving the nature and
2 evolution of the Bangong–Nujiang Tethyan Ocean: New perspectives from the
3 intraplate oceanic-island fragments preserved in Northern Tibet: GSA Bulletin,
4 <https://doi.org/10.1130/B37044.1>.

5

6 Supplemental Material

- 7 • **Text S1.** Analytical methods
- 8 • **Figure S1.** Photomicrograph of the fossils in the limestone of the Tarenben
9 ocean island ([this study](#)), and cathodoluminescence (CL) images of the
10 conodont fossils in the limestone of the Gufeng ocean island ([Fan et al., 2017](#))
- 11 • **Text S2 and Figure S2.** Age difference of initial formation of the trachyte and
12 the basalt in the modern intraplate ocean islands
- 13 • **Text S3 and Figure S3.** Locations of modern intraplate ocean islands that
14 contain phonolite, and the thickness of oceanic lithosphere that underlies each
15 of these islands
- 16 • **Table S1.** Bulk-rock major (wt.%) and trace element (ppm) data of the
17 magmatic rocks in the Nare intraplate ocean island fragment in the BNSZ
- 18 • **Table S2.** Bulk-rock major (wt.%) and trace element (ppm) data of the
19 magmatic rocks in the Gufeng intraplate ocean island fragment in the BNSZ
- 20 • **Table S3.** Bulk-rock major (wt.%) and trace element (ppm) data of the
21 magmatic rocks in the Maqiao intraplate ocean island fragment in the BNSZ
- 22 • **Table S4.** Bulk-rock major (wt.%) and trace element (ppm) data of the
23 magmatic rocks in the Tarenben intraplate ocean island fragment in the BNSZ
- 24 • **Table S5.** Bulk-rock major (wt.%) and trace element (ppm) data of the
25 magmatic rocks in the Zhonggang intraplate ocean island fragment in the
26 BNSZ
- 27 • **Table S6.** Zircon LA–ICP–MS U–Pb data of the magmatic rocks in the Nare
28 intraplate ocean island fragment in the BNSZ
- 29 • **Table S7.** Zircon LA–ICP–MS U–Pb data of the magmatic rocks in the
30 Maqiao intraplate ocean island fragment in the BNSZ

- 31 • **Table S8.** Zircon LA–ICP–MS U–Pb data of the magmatic rocks in the
32 Tarenben intraplate ocean island fragment in the BNSZ
- 33 • **Table S9.** Zircon LA–ICP–MS U–Pb data of the magmatic rocks in the
34 Zhonggang intraplate ocean island fragment in the BNSZ
- 35 • **Table S10.** Sphene LA–ICP–MS U–Pb data of the magmatic rocks in the
36 Zhonggang intraplate ocean island fragment in the BNSZ
- 37 • **Table S11.** Bulk-rock Sr–Nd isotopic composition of the magmatic rocks in
38 the intraplate ocean island fragment in the BNSZ

39

40 **Text S1. Analytical methods**

41 **1. Bulk–rock major and trace element analyses**

42 Samples were trimmed to remove weathered surfaces, cleaned with deionized
43 water, crushed, and powdered in an agate mill. Major element compositions were
44 analyzed by inductively coupled plasma–optical emission spectroscopy (ICP–OES;
45 Leeman Prodigy) with high-dispersion Echelle optics at the Key Laboratory of
46 Mineral Resources Evaluation in Northeast Asia, Ministry of Natural Resources of
47 China, Changchun, China. Loss on ignition (LOI) values were determined by heating
48 1 g of sample in a furnace at 1000 °C for several hours before being cooled in a
49 desiccator and reweighed. Analytical uncertainties for the major elements are <1 wt.%.
50 Trace element compositions were analyzed by inductively coupled plasma–mass
51 spectrometry (ICP–MS; Agilent–7900). The analytical accuracy and precision during
52 trace element analysis were determined from standards AGV–2 (US Geological
53 Survey standard) and GSR–3 (Chinese national geological reference standard). The
54 analytical accuracy is <5 wt.% for most elements. The values obtained for the
55 standards are in good agreement with recommended values ([Govindaraju, 1994](#)).

56

57 **2. Zircon U-Pb dating**

58 Zircon grains were separated by crushing, conventional heavy liquid and
59 magnetic techniques from sandstone samples in the Laboratory of the Geological
60 Team of Hebei Province, Langfang, China. The internal structures of zircon were
61 characterized using cathodoluminescence (CL) in the Continental Dynamics
62 Laboratory, Chinese Academy of Geological Sciences, Beijing, China to select spots
63 for laser ablation–inductively coupled plasma–mass spectroscopy (LA–ICP–MS)
64 analysis. LA–ICP–MS U–Pb zircon dating was carried out in the Key Laboratory of
65 Mineral Resources Evaluation in Northeast Asia, Ministry of Natural Resources of
66 China, Changchun, China. The spot size was 32 µm for each sample. Helium was
67 used as a carrier gas. Reference and internal zircon standards 91500 ([Wiedenbeck et](#)
68 [al., 1995](#)) and NIST610 (^{29}Si), respectively, were used for instrumental calibration.
69 The Pb correction method of [Anderson \(2002\)](#) was applied with analytical details

70 following Yuan et al. (2004). Reported uncertainties for the age analyses are given as
71 1σ values with weighted mean ages in the 95% confidence level. Isotopic data were
72 processed using the GLITTER (version 4.4) and Isoplot/Ex (version 3.0) programs
73 (Ludwig et al., 2003). The ages reported are $^{206}\text{Pb}/^{238}\text{U}$ ages for grains <1000 Ma and
74 $^{207}\text{Pb}/^{206}\text{Pb}$ ages for grains >1000 Ma. For statistical purpose, zircon ages with a
75 discordance of >10%, and those fall off the 1:1 age line was considered to be usable
76 (Spencer et al., 2016).

77

78 **3. Sphene U-Pb dating**

79 Sphene U-Pb dating analyses were conducted by LA-ICP-MS at Beijing
80 GeoAnalysis Technology Co., Ltd. Laser sampling was performed using a
81 RESOlution 193 nm laser ablation system. An Agilent 7500 ICP-MS instrument was
82 used to acquire ion-signal intensities. Helium was applied as a carrier gas. Argon was
83 used as the make-up gas and mixed with the carrier gas via a T-connector before
84 entering the ICP. Each analysis incorporated a background acquisition of
85 approximately 15-20 s (gas blank) followed by 45 s data acquisition from the sample.
86 Off-line raw data selection and integration of background and analyte signals, and
87 time-drift correction and quantitative calibration for U-Pb dating was performed by
88 *ICPMsDataCal* (Liu et al., 2010).

89 Titanite BLR-1 was used as external standard for U-Pb dating, and was analyzed
90 twice every 5-10 analyses. Time-dependent drifts of U-Th-Pb isotopic ratios were
91 corrected using a linear interpolation (with time) for every 5-10 analyses according to
92 the variations of BLR-1 (i.e., 2 titanite BLR-1 + 5-10 samples + 2 titanite BLR-1).
93 Uncertainty of preferred values for the external standard BLR-1 was propagated to the
94 ultimate results of the samples. Concordia diagrams and weighted mean calculations
95 were made using Isoplot/Ex_ver3.

96

97 **4. Bulk-rock Sr–Nd isotopes**

98 Bulk-rock Sr–Nd isotopic analyses were undertaken by Beijing Createch Testing
99 Technology Co., Ltd, Beijing. Prior to analysis, sample powders were dissolved in a

100 mixture of HF, HNO₃, and HClO₄ in Teflon bombs and separated by routine
101 cation-exchange techniques. Sr–Nd isotopic measurements were performed using a
102 Nu Plasma II MC–ICP–MS. Mass fractionation corrections and adjustments for
103 instrumental drift for Sr isotopic ratios were based on ⁸⁶Sr/⁸⁸Sr = 0.1194, and the
104 analyzed composition of the NIST SRM 987 isotopic standard, respectively. Mass
105 fractionation and instrumental drift corrections for Nd isotopic ratios were based on
106 ¹⁴⁶Nd/¹⁴⁴Nd = 0.7219, and the analyzed composition of the JNd-1 isotopic standard,
107 respectively.

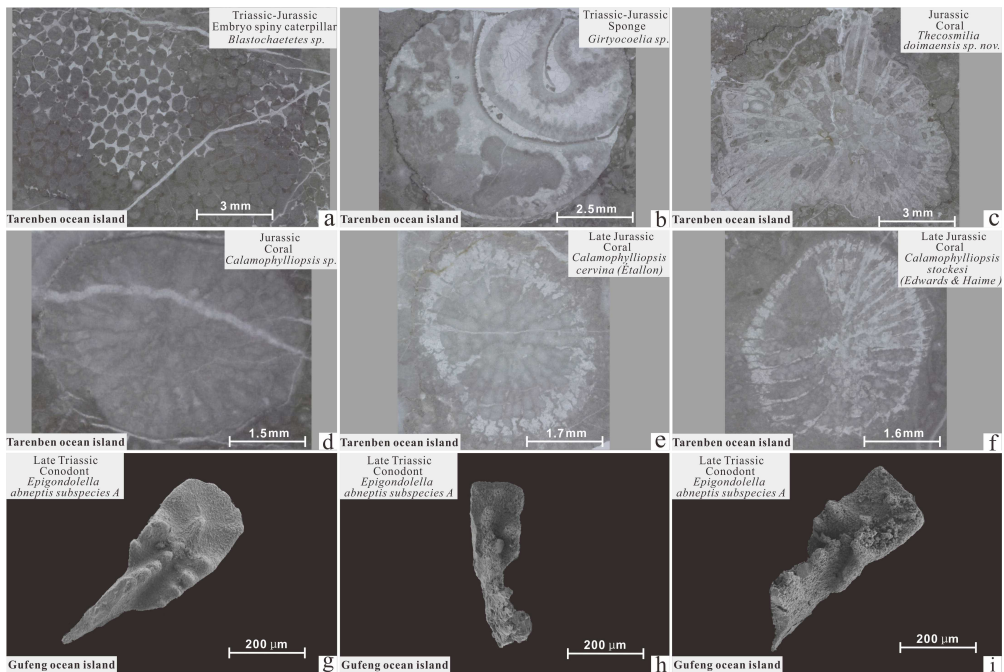
108

109

110 **References cited**

- 111 Anderson, T., 2002, Correction of common lead in U–Pb analyses that do not report
112 ²⁰⁴Pb: Chemical Geology, v. 192, p. 59–79.
- 113 Carl S, Johannes H, Peng S, Hannah H.W, Yi H, Eric R, Mark S. 2016. MKED1: A
114 new titanite standard for in situ analysis of Sm–Nd isotopes and U–Pb
115 geochronology. Chemical Geology, 425: 110-126
- 116 Goolaerts, A., Mattielli, N., de Jong, J., Weis, D., Scoates, J.S., 2004, Hf and Lu
117 isotopic reference values for the zircon standard 91500 by MC–ICP–MS:
118 Chemical Geology, v. 206, p. 1–9.
- 119 Govindaraju, K., 1994, Compilation of working values and sample description for 383
120 geostandards: Geostand. Newslett, v. 18, p. 1–158.
- 121 Hu, Z.C., Liu, Y.S., Gao, S., Liu, W.G., Zhang, W., Tong, X.R., Lin, L., Zong, K.Q.,
122 Li, M., Chen, H.H., Zhou, L., and Yang, L., 2012, Improved in situ Hf isotope
123 ratio analysis of zircon using newly designed X skimmer cone and Jet sample
124 cone in combination with the addition of nitrogen by laser ablation multiple
125 collector ICP–MS: Journal of Analytical Atomic Spectrometry, v. 27, p.
126 1391–1399.
- 127 Liu, Y.S., Gao, S., Hu, Z.C., Gao, C.G., Zong, K.Q., and Wang, D.B., 2010,
128 Continental and oceanic crust recycling–induced melt–peridotite interactions in
129 the Trans–North China Orogen: U–Pb dating, Hf isotopes and trace elements in
130 zircons from mantle xenoliths: Journal of Petrology, v. 51, p. 537–571.

- 131 Ludwig, K.J., 2003, ISOPLOT 3.0: Berkeley Geochronology Center Special
132 Publication, v. 4, p. 70.
- 133 Spencer, C.J., Kirkland, C.L., Taylor, R.J.M., 2016. Strategies towards statistically
134 robust interpretations of in situ U-Pb zircon geochronology. *Geoscience*
135 *Frontiers*, v. 7, p. 581–589.
- 136 Wiedenbeck, M., Allé, P., Corfu, F., Griffin, W.L., Meier, M., Oberli, F., Quadt, A.V.,
137 Roddick, J.C., and Spiegel, W., 1995, Three natural zircon standards for
138 U-Th-Pb, Lu-Hf, trace element and REE analyses: *Geostandards and*
139 *Geoanalytical Research*, v. 19, p. 1–23.
- 140 Woodhead, J., Hergt, J., Shelley, M., Eggins, S., and Kemp, R., 2004, Zircon
141 Hf-isotope analysis with an excimer laser, depth profiling, ablation of complex
142 geometries, and concomitant age estimation: *Chemical Geology*, v. 209, p.
143 121–135.
- 144 Yuan, H.L., Gao, S., Liu, X.M., Li, H.M., Günther, D., and Wu, F.Y., 2004, Accurate
145 U-Pb age and trace element determinations of zircon by laser
146 ablation-inductively coupled plasma mass spectrometry: *Geostandards and*
147 *Geoanalytical Research*, v. 28, p. 353–370.
- 148
- 149



150

151 **Figure S1.** Photomicrograph of the fossils in the limestone of the Tarenben ocean
 152 island ([this study](#)), and cathodoluminescence (CL) images of the conodont fossils
 153 in the limestone of the Gufeng ocean island ([Fan et al., 2017](#))

154 **References cited**

155 Fan, J.J., Li, C., Wang, M., Liu, Y.M., and Xie, C.M., 2017, Remnants of a Late
 156 Triassic ocean island in the Gufeng area, northern Tibet: Implications for the
 157 opening and early evolution of the Bangong–Nujiang Tethyan Ocean: Journal
 158 of Asian Earth Sciences, v. 135, p. 35–50.

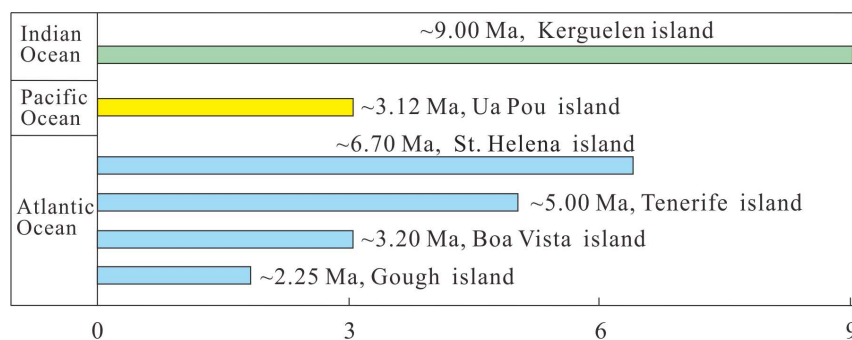
159

160

161 **Text S2. Age difference of initial formation of the trachyte and the basalt in the
 162 modern intraplate ocean islands**

163 We summarize the chronology of magmatic rocks in the modern intraplate ocean
 164 islands, and found that the initial formation age of the trachyte is usually 2–9 Ma later
 165 than that of the early basalts, for examples, the basalt of the Gough island in the
 166 Atlantic Ocean initially erupted at ~2.55 Ma, and the trachyte initially erupted at ~0.3
 167 Ma, thus the age difference is ~2.25 Ma ([Maund et al., 1988](#)); the basalt of the Boa
 168 Vista island in the Atlantic Ocean initially erupted at ~17.5 Ma, and the trachyte

169 initially erupted at ~14.3 Ma, thus the age difference is ~3.2 Ma (Ancochea et al.,
170 2012); the basalt of the Tenerife island in the Atlantic Ocean erupted at ~8.5 Ma, and
171 the trachyte initially erupted at ~3.5 Ma, thus the age difference is ~5 Ma (Carracedo
172 et al., 2002); the basalt of the St Helena island in the Atlantic Ocean initially erupted
173 at ~14.3 Ma, and the trachyte initially erupted at ~7.6 Ma, thus the age difference is
174 ~6.7 Ma (Baker, 1969); the basalt of the Ua Pou island in the Pacific Ocean initially
175 erupted at ~5.61 Ma, and the trachyte initially erupted at ~2.49 Ma, thus the age
176 difference is ~3.12 Ma (Legendre et al., 2005); the basalt of the Kerguelen islands in
177 the Indian Ocean initially erupted at ~34 Ma, and the trachyte initially erupted at ~25
178 Ma, thus the age difference is ~9 Ma (Nicolaysen et al., 2000; Frey et al., 2000, 2002).



179
180 Figure S2 Age difference of initial formation of the trachyte and the basalt in the
181 modern intraplate ocean islands

182 **References cited**

- 183 Maund, J.G., Rex, D.C., Le Roex, A.P., and Reid, D.L., 1988. Volcanism on Gough
184 Island: a revised stratigraphy. Geological Magazine, v. 125, p. 175–181.
- 185 Ancochea, E., Hernan, F., Huertas, M.J., et al., 2012. A Basic Radial Dike Swarm of
186 Boa Vista (Cape Verde Archipelago); Its Significance in the Evolution of the
187 Island. Journal of Volcanology and Geothermal Research, v. 243–244, p. 24–37.
- 188 Carracedo, J.C., Pe'rez Torrado, F.J., Ancochea, E., Meco, J., Herna'n, F., Cubas, C.R.,
189 Casillas, R., Rodri'guez Badiola, E. & Ahijado, A., 2002. Cenozoic volcanism
190 II: the Canary Islands. The geology of Spain (ed. by W. Gibbons and T.
191 Moreno), pp. 439–472. The Geological Society, London.
- 192 Baker, I., Petrology of the Volcanic Rocks of Saint Helena Island, South Atlantic.
193 Geological Society of America Bulletin, v. 80, p. 1283-1310.

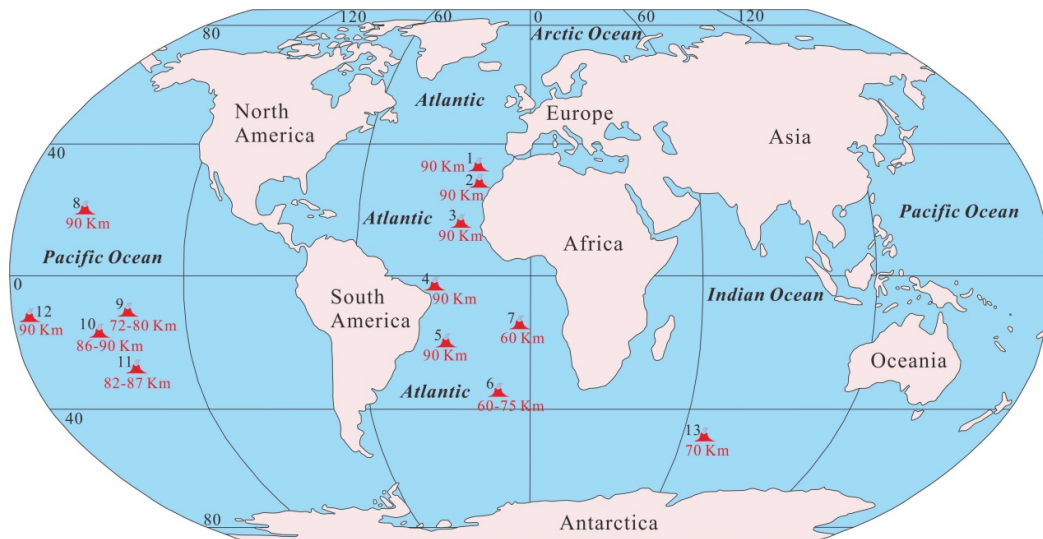
- 194 Legendre, C., Maury, R.C., Caroff, M., et al., 2005. Origin of Exceptionally Abundant
195 Phonolites on Ua Pou Island (Marquesas, French Polynesia): Partial Melting of
196 Basanites Followed by Crustal Contamination. *Journal of Petrology*, v. 46 (9), p.
197 1925–1962.
- 198 Nicolaysen, K., Frey, F.A., Hodges, K.V., Weis, D., Giret, A., 2000. $^{40}\text{Ar}/^{39}\text{Ar}$
199 geochronology of flood basalts from the Kerguelen Archipelago, southern
200 Indian Ocean: implications for Cenozoic eruption rates of the Kerguelen plume.
201 *Earth and Planetary Science Letters*, v. 174, p. 313–328.
- 202 Frey, F.A., Weis, D., Yang, H.J., Nicolaysen, K., Leyrit, H., Giret, A., 2000. Temporal
203 geochemical trends in the Kerguelen archipelago basalts: evidence for
204 decreasing magma supply from the Kerguelen plume. *Chemical Geology*, v. 164,
205 p. 61–80.
- 206 Frey, F.A., Nicolaysen, K.A., Kubit, B.K., Weis, D., Giret, A., 2002. Flood basalts
207 from Mont Tourmente in the central Kerguelen Archipelago: the change from
208 tholeiitic/transitional to alkali basalts at 25 Ma. *Journal of Petrology*, v. 43, p.
209 1367–1387.
- 210

211 **Text S3. Locations of modern intraplate ocean islands that contain phonolite, and**
212 **the thickness of oceanic lithosphere that underlies each of these islands**

213 Phonolite is a relatively rare rock type in nature, and it makes up only one
214 thousandth of the volume of extrusive volcanic rocks. Phonolite is also rare in modern
215 ocean islands, as it was indicated by that although there are tens of thousands of
216 modern ocean islands, very few have been reported to contain phonolite.

217 In present-day ocean basins, the intraplate ocean islands that contain phonite
218 include: Hawaii, Marquesas, Society, Samoa, Raevavae and Tubuai in the Pacific
219 Ocean, the Selvagen, Canary, Cape Verde, Fernando de noronha, Trindade, St Helena,
220 Tristan da Cunha in the Atlantic Ocean, and the Kerguelen in the Indian Ocean. The
221 common features of the above-mentioned intraplate ocean islands are that when the
222 phonite erupted, the intraplate ocean islands was on the thick oceanic lithosphere, for
223 examples, the oceanic lithospher under the Hawaii, Selvagen, Canary, Cape Verde,

224 Fernando de noronha, Trinidad is ~90Km when the phonite erupted; the oceanic
225 lithosphere under the Marquesas, Society, Samoa, Raevavae, Tubuai, St Helena, Tristan
226 da Cunha, and Kerguelen is 60~90Km when the phonite erupted ([Clouard et al., 2004](#);
227 [Humphreys and Niu, 2009](#); [Bonadio et al., 2018](#)).



228 Island Group: 1, Selvagens; 2, Canary; 3, Cape Verde; 4, Fernando de noronha; 5, Trinidad; 6, Tristan da Cunha; 7, St Helena;
229 8, Hawaiian; 9, Marquesas; 10, Society; 11, Raivavae-Tubuai; 12, Samoan; 13, Kerguelen;
230 “90 Km” represents the thickness of the oceanic lithosphere under the intraplate ocean islands

231
232 Figure S3 Locations of modern intraplate ocean islands that contain phonolite, and the
233 thickness of oceanic lithosphere that underlies each of these islands

234 **References cited**

- 235 Humphreys, E.R., and Niu, Y., 2009. On the composition of ocean island basalts
236 (OIB): the effects of lithospheric thickness variation and mantle metasomatism.
237 Lithos, v. 112, p. 118–136.
- 238 Clouard, V., Bonneville, A., 2004a. Ages of seamounts, islands and plateaus on the
239 Pacific Plate. version 2.1 www.mantleplumes.org.
- 240 Bonadio, R., Geissler, W.H., Lebedev, S., Fullea, J., Matteo, R., Celle, N.L., Jokat, W.,
241 Jegen, M., Sens-Schonfelder, C., and Baba, K., 2018. Hot Upper Mantle Beneath
242 the Tristan da Cunha Hotspot From Probabilistic Rayleigh-Wave Inversion and
Petrological Modeling. Geochemistry, Geophysics, Geosystems, v. 19, p.
1412–1428.

Table S1 Bulk-rock major (wt.%) and trace element (ppm) data of the magmatic rocks in the Nare ocean island fragment in the BNSZ

Sample	B21T61H1	B21T61H2	B21T61H3	B21T61H4	B21T61H5	B21T61H6	B21T61H7	B21T61H8	B21T61H9	NH1	NH2	NH3	NH4	NH5
Lithology	Trachyte	Trachyte	Trachyte	Trachyte	Trachyte	Trachyte	Trachyte	Trachyte	Trachyte	Basalt	Basalt	Basalt	Basalt	Basalt
Reference	This study									Fan et al., 2018				
SiO ₂	62.1	63.6	63.8	63.4	63.1	63.4	62.9	63.8	62.8	45.1	47.5	51.2	50.6	52.1
TiO ₂	0.20	0.19	0.19	0.20	0.20	0.20	0.20	0.19	0.20	3.31	3.05	2.9	3.25	2.93
Al ₂ O ₃	19.3	17.6	18.3	18.7	17.9	17.6	17.3	17.8	17.8	12.1	12.5	10.4	10.9	10.3
Fe ₂ O _{3T}	5.06	5.17	5.14	5.33	4.97	5.42	5.40	5.32	5.34	11.5	11.4	9.14	10.5	11.1
MnO	0.06	0.12	0.08	0.09	0.06	0.11	0.14	0.07	0.15	0.15	0.16	0.13	0.13	0.15
MgO	0.32	0.13	0.20	0.17	0.14	0.12	0.15	0.12	0.13	5.63	7.47	4.41	5.12	5.51
CaO	0.14	0.91	0.15	0.20	0.63	0.51	1.12	0.66	0.62	12.1	7.61	11.5	8.45	8.06
Na ₂ O	7.74	8.10	6.28	6.81	5.86	6.65	7.42	8.26	6.06	3.09	3.59	3.44	3.76	3.34
K ₂ O	2.96	2.27	3.77	3.47	5.49	4.08	3.33	2.17	5.20	1.85	1.14	1.23	1.31	1.32
P ₂ O ₅	0.05	0.06	0.06	0.06	0.04	0.05	0.03	0.06	0.06	0.47	0.44	0.36	0.37	0.33
LOI	1.58	1.65	1.52	1.55	1.48	1.44	1.81	1.3	1.55	3.32	4.02	4.66	5.06	4.29
Sc	2.61	2.58	3.33	3.05	2.54	4.73	2.96	2.71	2.81	26.4	28.9	24.5	27.4	26.4
V	12.4	7.07	10.7	10.4	2.97	9.64	2.90	11.64	11.61	300	323	291	332	307
Cr	8.02	5.10	6.46	24.1	7.03	6.69	7.78	12.3	6.99	235	234	178	197	240
Co	0.84	0.26	0.29	0.53	0.29	0.32	0.40	0.51	0.35	45.6	45.1	42.4	40.9	39.4
Ni	9.55	2.85	3.16	10.64	1.93	4.05	2.82	5.83	3.51	111	101	84.5	74.4	85.1
Cu	1.96	1.58	1.53	1.62	2.23	2.26	1.97	2.31	3.55	98.7	103	91.3	105	90.8
Ga	41.7	32.8	36.2	36.8	37.6	35.1	34.1	37.2	37.2	20.7	21.2	18.3	20.5	20.6
Rb	119	62.2	112	98.5	144	100	80.9	75.4	143	36.9	23.3	24	27.1	24.3
Sr	21.1	27.1	22.5	23.4	31.6	29.2	31.6	24.4	29.2	223	180	223	200	161
Y	55.5	75.0	68.3	68.0	81.2	73.1	67.5	75.9	69.4	27.2	27.6	24.6	28.7	25.5

	866	1208	1303	1227	1204	1230	1144	1298	1243	218	234	204	240	209
Nb	196	209	213	208	208	210	202	220	217	33.9	23.9	40.8	48	42.1
Cs	2.73	0.85	1.69	1.50	1.42	1.23	1.08	0.82	1.31	0.73	0.73	0.4	1.03	0.79
Ba	48.3	89.0	109	104	177	183	269	63.3	261	231	738	192	191	347
La	128	120	118	107	126	115	116	130	124	26.3	28.9	24.1	31.4	23
Ce	220	221	219	208	229	210	207	246	228	62.5	65.7	54.3	67.7	53.4
Pr	25.3	24.0	24.0	22.0	24.5	23.4	23.1	26.0	24.9	8.01	8.36	6.95	8.46	6.91
Nd	83.7	83.6	82.6	76.7	85.9	82.3	80.1	90.7	87.3	35.1	36.6	31.7	37.9	31.6
Sm	14.5	16.1	15.6	14.7	16.7	16.0	15.5	17.1	16.5	8.21	8.49	7.36	8.57	7.49
Eu	1.92	2.11	2.04	1.92	2.14	2.14	2.14	2.19	2.21	2.67	2.87	2.41	2.81	2.45
Gd	13.2	15.3	15.3	14.3	16.3	15.3	14.7	16.9	15.9	8.11	8.43	7.37	8.54	7.43
Tb	2.08	2.48	2.44	2.33	2.61	2.41	2.31	2.64	2.46	1.14	1.18	1	1.17	1.03
Dy	12.0	14.8	14.4	13.7	15.3	14.2	13.3	15.2	14.1	6.24	6.5	5.6	6.51	5.74
Ho	2.38	3.01	2.88	2.72	3.00	2.82	2.61	2.92	2.79	1.1	1.14	0.96	1.12	0.99
Er	6.66	8.49	8.17	7.66	8.44	7.92	7.42	8.26	7.97	2.8	2.94	2.49	2.92	2.55
Tm	0.97	1.23	1.21	1.13	1.22	1.17	1.08	1.20	1.18	0.35	0.36	0.3	0.36	0.31
Yb	6.39	7.79	7.55	7.14	7.52	7.34	6.73	7.50	7.46	2.05	2.19	1.84	2.16	1.88
Lu	0.92	1.14	1.14	1.06	1.11	1.06	1.01	1.13	1.10	0.27	0.29	0.24	0.28	0.25
Hf	23.6	25.9	26.4	25.8	25.2	25.6	24.5	27.2	26.2	5.27	5.63	5.24	6.1	5.31
Ta	13.6	12.7	13.1	13.0	12.5	12.8	12.4	13.3	13.1	2.68	1.35	2.5	2.96	2.59
Pb	4.63	4.43	3.44	3.46	4.47	5.49	4.53	4.06	6.79	2.28	3.32	1.76	2.2	1.97
Th	14.3	12.6	12.8	13.4	13.9	13.3	13.2	14.4	14.3	3.27	3.42	2.89	3.39	2.88
U	0.70	0.66	1.29	1.26	0.86	1.09	1.17	0.88	0.69	0.87	1.09	0.6	1.04	0.63

Continued Table S1

Sample	NH6	NH7	NH8	NH9	NH10	NH11	NH12	NH13	NH14	NH15	NH16	NH17	NH18	NH19	NH20
Lithology	Trachyte	Trachyte	Trachyte	Trachyte	Trachyte	Trachyte	Trachyte	Trachyte	Trachyte	Trachyte	Trachyte	Trachyte	Trachyte	Trachyte	Trachyte
Reference	Fan et al., 2018														
SiO ₂	62.8	60.3	62.1	64	61.8	62.3	61.6	62.1	61.5	65.3	64.6	63.3	64.1	63.9	64.6
TiO ₂	0.18	0.2	0.19	0.18	0.2	0.19	0.2	0.19	0.19	0.17	0.15	0.16	0.16	0.17	0.17
Al ₂ O ₃	18.5	19.1	19	18.4	19.3	18.4	18.8	18.8	18.4	16.8	16.9	17.6	17.3	17.8	17
Fe ₂ O _{3T}	4.95	5.24	4.8	4.51	4.85	5.16	5.37	5.2	5.34	4.73	4.78	5.16	4.89	5.19	5.22
MnO	0.09	0.14	0.1	0.1	0.1	0.09	0.13	0.09	0.13	0.09	0.07	0.09	0.08	0.09	0.1
MgO	0.16	0.19	0.18	0.15	0.18	0.14	0.15	0.25	0.21	0.11	0.17	0.14	0.14	0.14	0.12
CaO	0.3	0.59	0.14	0.12	0.28	0.31	0.23	0.11	0.3	0.93	1.03	0.77	0.93	0.39	0.49
Na ₂ O	6.12	6.41	7.05	8.02	8.27	6.61	7.09	6.18	6.37	7.02	7.01	7.14	6.86	6.67	6.83
K ₂ O	4.76	5.1	4.11	2.85	3.16	4.92	4.63	5.19	5	2.87	2.93	3.76	3.47	4.00	3.78
P ₂ O ₅	0.05	0.06	0.06	0.03	0.04	0.06	0.06	0.05	0.05	0.04	0.06	0.05	0.04	0.04	0.05
LOI	1.34	1.76	1.49	1.08	1	0.99	0.9	1.12	1.69	1.54	1.91	1.5	1.64	1.31	1.26
Sc	2.04	2.14	1.99	1.85	2	2.09	1.95	2.09	2.1	1.84	1.81	1.91	2	2.13	2.03
V	16.2	20	10.3	1.87	1.77	7.24	7.62	4.67	6.44	3.02	6.5	5.82	3.78	7.22	6.92
Cr	3.01	3.08	2.75	5.53	5.33	7.59	5.19	2.62	1.65	4.76	3.19	1.27	2.32	3.36	1.27
Co	0.15	1.15	0.12	0.11	0.13	0.13	0.15	0.17	0.11	0.28	0.35	0.19	0.2	0.37	0.38
Ni	5.96	5.51	2.46	6.05	3.01	4.8	3.36	7.19	0.43	2.54	4.18	2.83	1.96	2.35	2.93
Cu	0.49	1.46	6.3	1.28	1.02	1.28	0.74	1.08	0.83	0.58	3.8	1.48	1.65	1.56	2.13
Ga	36.3	38.9	35.8	33.2	34.9	40.2	38.1	41.7	42.2	33.7	30.4	37.8	36.4	40.6	36.5
Rb	122	136	80.8	56.8	62.9	154	138	176	169	97.2	46.4	89.6	69.7	86.8	64.3
Sr	26.3	27.5	45.2	38.6	41.9	26.2	27.6	30.3	32.9	48.3	27.7	27.7	31.3	21.3	34.4
Y	86.2	67.6	75.3	62.7	77.5	84.5	76.3	80.6	82.3	79.3	52	56.9	56.6	62.7	59.5

	1073	1031	1077	927	1079	1122	1049	1117	1114	1047	927	1022	1008	1093	1046
Nb	209	209	182	192	206	221	213	226	225	210	172	204	209	256	201
Cs	1.43	1.79	0.84	0.86	1.24	1.82	1.77	1.99	1.99	1.52	0.79	1.25	0.99	1.06	0.94
Ba	181	178	167	147	162	193	202	195	210	135	133	124	113	153	150
La	130	131	133	141	133	139	132	138	139	131	101	103	99	106	103
Ce	251	252	248	262	258	267	255	265	265	242	185	190	181	201	191
Pr	26.8	26.3	26.4	27.8	27.2	28.3	26.7	28.2	28	25.9	21.4	22.2	21.4	23.2	21.9
Nd	96.5	94.1	93.2	99.1	97.3	102	95.6	101	100	92	69.7	73.3	70.2	76.4	70
Sm	18.6	17.9	17.7	17.9	18.9	19.7	18.4	19.1	19.3	17.6	12.4	13.8	13.4	14.6	12
Eu	2.41	2.39	2.33	2.3	2.42	2.52	2.41	2.57	2.5	2.26	1.67	1.79	1.72	1.9	1.53
Gd	17.2	16	16.7	15.8	17.3	18.1	16.8	17.3	17.7	16.1	11.6	12.5	12.4	13.5	11.1
Tb	2.69	2.41	2.61	2.33	2.66	2.83	2.6	2.68	2.76	2.52	1.99	2.15	2.12	2.35	1.99
Dy	16.4	14.1	15.5	13.4	15.7	16.8	15.4	16	16.4	15.4	11.5	12.4	12.1	13.5	11.9
Ho	3.2	2.65	2.94	2.5	2.99	3.21	2.95	3.13	3.14	3.01	2.36	2.58	2.45	2.77	2.52
Er	9.42	7.61	8.44	7.16	8.62	9.21	8.44	9.2	9.15	8.81	6.35	7	6.59	7.41	6.8
Tm	1.32	1.09	1.19	1.02	1.22	1.28	1.18	1.32	1.28	1.25	0.91	1.01	0.95	1.05	0.98
Yb	8.59	7.1	7.82	6.81	7.96	8.32	7.76	8.58	8.32	8.14	5.93	6.47	6.08	6.74	6.26
Lu	1.2	1.01	1.1	0.98	1.13	1.17	1.09	1.19	1.17	1.14	0.83	0.91	0.86	0.96	0.89
Hf	24.7	25.2	25	22.4	25.4	26.8	25.3	26	26.9	24.4	20.8	22.7	22	23.8	22.1
Ta	13	13.7	13.4	13.3	14.1	14.8	13.8	14.4	14.8	13	11.8	13.1	12.3	16	13.1
Pb	4.92	5.23	8.32	5.06	6.15	6.08	5.96	7.37	7.36	5.9	2.06	3.82	4.63	2.85	2.43
Th	20	20.4	20	20.3	20.7	21.3	20.1	21	21.5	19.3	13.6	14	13.5	14.8	13.7
U	1.55	1.78	2.13	1.88	2.7	1.46	1.38	1.54	1.5	1.31	0.99	1.07	0.94	1.04	0.97

247

References cited

248

Fan, J.J., Li, C., Liu, J.H., Wang, M., Liu, Y.M., Xie, C.M., 2018. The Middle Triassic evolution of the Bangong–Nujiang Tethyan Ocean: evidence from analyses of OIB-type basalts and OIB-derived phonolites in northern Tibet. International Journal of Earth

249

Sciences, v. 107, p. 1755–1775.

Table S2 Bulk-rock major (wt.%) and trace element (ppm) data of the magmatic rocks in the Gufeng ocean island fragment in the BNSZ

Sample	DT13T6H8	DT13T6H9	DT13T6H10	G3H1	G3H2	G3H3	G3H4	G3H5	G3H6	G3H7
Lithology	Trachyandesite	Trachyandesite	Trachyandesite	Basalt	Basalt	Basalt	Basalt	Basalt	Basalt	Basalt
Reference	This study				Fan et al., 2017					
SiO ₂	51.8	52.4	53.1	47.0	49.4	44.3	43.6	45.5	44.9	45.2
TiO ₂	2.28	2.37	2.32	2.46	2.44	2.52	2.54	2.45	2.64	2.41
Al ₂ O ₃	10.6	12.1	12.5	14.8	14	15.1	13.6	12.5	14.6	16.4
Fe ₂ O _{3T}	8.33	9.70	9.47	11.6	10.7	10.4	12.3	11.8	11.9	12.6
MnO	0.11	0.11	0.11	0.11	0.1	0.14	0.17	0.18	0.15	0.13
MgO	4.06	3.82	3.81	4.28	3.95	4.07	6.67	6.92	5.63	4.66
CaO	10.94	8.36	8.11	8.9	8.09	10	10.4	10.8	8.89	6.79
Na ₂ O	3.57	4.23	4.53	4.83	5.24	5.15	3.92	3.82	4.28	5.4
K ₂ O	0.47	0.50	0.43	1.08	1.24	0.34	0.37	0.32	0.74	1.44
P ₂ O ₅	0.35	0.42	0.45	0.46	0.44	0.56	0.48	0.46	0.52	0.56
LOI	6.82	5.32	4.47	3.65	3.52	5.75	4.28	3.86	4.3	3.82
Sc	31.2	21.1	21.1	15.7	17.7	16.9	30.8	26.9	26.2	14.1
V	282	300	267	276	288	294	271	305	322	330
Cr	160	38.8	44.6	10.3	11.4	14.6	245	172	38.2	6.69
Co	42.4	37.2	35.8	34.4	30.1	35.9	40.2	44.9	37.7	34.2
Ni	72.3	62.8	50.4	55.9	53.1	42.4	107	130	69	54.5
Cu	81.8	55.7	53.3	67.7	57.4	80.3	24.7	51.8	70	78
Ga	19.4	23.6	22.6	23.1	22.4	23.2	22.7	24.8	26.2	26.1
Rb	13.1	22.0	15.9	49	69.7	9.48	9.52	12.5	29.2	81.9
Sr	325	310	351	314	356	517	290	322	278	374
Y	17.9	20.1	20.1	19.8	19.9	21.5	19.5	22.2	21.8	21.6

Zr	176	193	187	204	210	187	179	197	198	186
Nb	40.8	48.6	50.1	44	43.2	37.6	31.4	35.3	35	63.6
Cs	1.83	3.64	1.85	6.65	8.54	0.96	1.06	1.87	3.16	8.61
Ba	1055	441	468	558	576	476	360	559	828	571
La	22.7	28.0	28.9	28.3	29.7	32.7	26	32.6	28.7	27
Ce	49.4	60.6	61.4	61.6	62.7	71.4	58.8	71.1	65.4	59.1
Pr	6.09	7.37	7.47	7.72	7.8	8.67	7.31	8.61	8.16	7.53
Nd	26.9	32.0	32.4	31.8	32.4	36	31.4	36.3	35	30.5
Sm	6.06	6.96	6.96	6.8	6.96	7.71	7.03	7.91	7.75	6.6
Eu	2.08	2.28	2.33	2.25	2.31	2.56	2.3	2.67	2.57	2.15
Gd	5.84	6.52	6.59	6.38	6.51	7.28	6.74	7.47	7.44	6.1
Tb	0.78	0.86	0.86	0.83	0.85	0.97	0.91	1.01	1	0.85
Dy	4.20	4.63	4.64	4.51	4.58	5.1	4.8	5.33	5.28	4.33
Ho	0.70	0.78	0.78	0.77	0.79	0.88	0.81	0.9	0.91	0.78
Er	1.80	2.01	2.01	1.94	1.97	2.22	2.02	2.29	2.29	1.94
Tm	0.22	0.25	0.25	0.24	0.24	0.28	0.25	0.28	0.28	0.25
Yb	1.31	1.48	1.49	1.46	1.48	1.66	1.51	1.68	1.68	1.5
Lu	0.18	0.20	0.20	0.2	0.2	0.22	0.2	0.23	0.23	0.21
Hf	4.49	4.64	4.57	5.12	5.26	4.49	4.45	4.8	4.82	3.93
Ta	2.52	2.94	3.09	2.57	2.52	2.1	2.03	2.36	2.36	3.95
Pb	3.00	2.27	1.98	7.06	1.82	3.44	2.21	1.52	8.47	1.69
Th	3.01	3.65	3.85	4.1	4.09	4.56	3.7	4.21	4.14	4.66
U	1.62	1.28	1.41	0.81	0.92	1.6	0.91	0.85	0.72	1.05

251

References cited

252

Fan, J.J., Li, C., Wang, M., Liu, Y.M., Xie, C.M., 2017. Remnants of a Late Triassic ocean island in the Gufeng area, northern Tibet: Implications for the opening and early evolution of the Bangong–Nujiang Tethyan Ocean. Journal of Asian Earth Sciences, v. 135, p.

253

35–50.

Table S3 Bulk-rock major (wt.%) and trace element (ppm) data of the magmatic rocks in the Maqiao ocean island fragment in the BNSZ

Sample	B21T28H4	B21T28H5	B21T28H6	B19T27H2	B19T38H1	SHT42H1	B19T30H3	SHT42H2	B19T30H1	B19T30H2
Lithology	Basalt	Basalt	Basalt	Trachyandesite	Trachyte	Trachyte	Trachyte	Phonolite	Phonolite	Phonolite
Reference	This study									
SiO ₂	47.9	49.0	47.0	53.8	59.7	59.2	61.9	58.6	58.5	58.3
TiO ₂	2.54	2.60	2.75	1.78	0.26	0.26	0.13	0.26	0.13	0.13
Al ₂ O ₃	12.1	12.0	12.2	16.6	18.8	18.5	19.6	18.6	19.3	19.4
Fe ₂ O _{3T}	11.8	11.3	12.6	9.29	4.80	4.76	3.86	5.62	6.06	5.74
MnO	0.17	0.16	0.18	0.29	0.13	0.13	0.10	0.16	0.15	0.13
MgO	7.73	7.52	8.37	2.35	0.85	0.94	0.59	1.04	0.94	0.86
CaO	12.1	10.7	11.8	5.21	2.76	2.40	2.52	2.74	3.32	4.23
Na ₂ O	2.83	3.46	2.50	5.59	6.49	6.33	7.78	6.76	7.01	7.03
K ₂ O	0.16	0.25	0.14	0.94	4.21	4.86	2.57	3.71	2.36	2.19
P ₂ O ₅	0.27	0.30	0.27	0.55	0.08	0.09	0.02	0.09	0.03	0.03
LOI	2.06	2.17	2.10	4.79	2.62	2.07	1.54	2.21	2.36	2.65
Sc	11.4	16.3	27.9	8.58	2.73	3.65	1.00	2.13	1.16	1.03
V	405	379	422	38.4	7.62		1.25		1.42	1.43
Cr	379	373	393	4.19	11.72	5.75	2.13	3.66	13.7	10.3
Co	44.8	46.5	46.3	11.8	1.04	1.16	0.29	1.57	0.52	0.46
Ni	118	118	122	4.32	4.47	1.79	0.78	2.61	6.87	5.16
Cu	94.9	129	109	7.64	9.35	10.4	19.9	10.6	4.51	7.27
Ga	19.5	16.9	20.0	19.9	24.8	27.4	21.5	29.8	24.2	25.9
Rb	3.04	3.71	2.19	19.9	32.0	22.7	33.4	15.7	30.7	29.8
Sr	659	364	601	429	168	175	119	140	185	182
Y	20.1	21.6	22.4	45.0	51.7	51.2	85.7	41.8	112.69	96.7

Zr	133	140	140	429	654	904	1389	882	1604	1466
Nb	14.0	14.6	14.6	113	171	209	347	154	418	387
Cs	0.32	0.44	0.35	2.09	1.30	1.38	0.42	1.58	0.35	0.33
Ba	38.7	58.5	51.2	553	1159	1195	825	990.1	817	790
La	13.4	13.6	13.7	91.4	73.3	60.3	274	48.7	290	334
Ce	33.3	34.0	35.6	176	153	118	423	108	500	507
Pr	4.487	4.58	4.69	20.5	18.5	15.7	39.2	13.3	47.4	46.4
Nd	19.9	20.5	21.1	72.3	67.8	57.4	120	49.9	147	142
Sm	5.04	5.24	5.26	14.2	13.6	11.7	18.3	10.2	23.2	21.0
Eu	1.73	1.89	1.89	4.40	2.81	2.59	0.95	2.33	1.16	1.23
Gd	5.29	5.54	5.77	11.9	11.8	10.7	15.1	9.36	20.3	18.4
Tb	0.79	0.84	0.86	1.69	1.92	1.67	2.62	1.48	3.28	2.88
Dy	4.46	4.67	4.80	9.73	10.8	9.82	15.4	8.72	19.0	16.9
Ho	0.85	0.87	0.91	1.92	2.23	1.98	3.36	1.73	4.12	3.66
Er	2.14	2.27	2.33	5.04	6.16	5.83	10.0	5.03	12.2	10.8
Tm	0.28	0.30	0.31	0.78	1.00	0.83	1.72	0.73	2.11	1.86
Yb	1.65	1.69	1.74	4.55	6.03	5.47	11.0	4.66	13.1	11.7
Lu	0.23	0.23	0.24	0.68	0.95	0.82	1.72	0.70	2.04	1.83
Hf	3.45	4.36	3.70	10.3	16.1	16.9	35.2	16.9	39.9	36.9
Ta	0.55	0.57	0.59	6.70	9.32	9.56	26.6	6.05	30.7	27.9
Pb	3.10	2.88	3.08	6.91	11.8	9.94	32.4	8.41	25.4	30.8
Th	0.54	0.59	0.68	10.7	15.91	11.5	75.0	7.43	91.8	80.9
U	0.26	0.32	0.33	2.80	3.42	3.46	13.8	3.05	17.8	16.1

Table S4 Bulk-rock major (wt.%) and trace element (ppm) data of the magmatic rocks in the Tarenben ocean island fragment in the BNSZ

Sample	B21T68H1	B21T68H2	B21T68H3	B21T69H1	B21T69H2	B21T69H3	B21T70H1	B21T70H2	B21T70H3
Lithology	Basalt	Basalt	Basalt	Basalt	Basalt	Basalt	Basalt	Basalt	Basalt
Reference	This study								
SiO ₂	44.7	44.4	45.2	45.3	43.4	43.8	46.1	46.0	45.9
Al ₂ O ₃	15.6	15.2	15.2	14.4	14.0	14.2	15.0	15.5	15.0
Fe ₂ O ₃ T	11.3	10.7	10.3	12.3	11.9	12.1	10.7	11.5	11.2
CaO	9.84	11.0	11.3	9.61	13.2	12.2	12.0	10.1	11.7
MgO	6.45	5.43	5.28	7.84	5.99	6.48	4.50	5.61	4.77
K ₂ O	0.50	0.60	0.64	0.42	0.29	0.48	0.13	0.20	0.15
Na ₂ O	3.80	4.07	4.16	3.52	3.45	3.41	4.23	4.18	4.14
TiO ₂	1.59	1.61	1.51	2.04	2.01	2.05	1.90	1.92	1.90
P ₂ O ₅	0.16	0.16	0.16	0.20	0.20	0.21	0.18	0.18	0.18
MnO	0.13	0.14	0.14	0.14	0.14	0.14	0.11	0.14	0.12
LOI	5.55	6.32	6.20	4.20	5.13	4.83	4.91	4.60	4.65
Li	23.3	20.9	18.6	26.6	18.4	22.1	18.3	34.7	20.2
Be	0.63	0.68	0.67	0.69	0.66	0.68	0.51	0.59	0.59
B	18.1	16.7	17.4	15.5	22.2	18.7	30.5	20.2	30.7
Sc	29.4	30.4	27.9	21.0	31.1	27.0	28.6	25.9	22.8
V	268	276	262	304	311	319	280	290	279
Cr	179	195	205	345	329	303	145	143	142
Co	48.1	48.6	44.2	54.3	52.5	51.7	48.9	46.0	46.8
Ni	98.5	104.4	101.8	158.2	143.1	136.4	78.8	74.1	74.8
Cu	85.0	87.5	85.2	78.1	78.9	80.6	79.1	79.1	75.4
Zn	88.6	92.1	83.3	83.9	80.4	84.0	85.4	83.0	88.2

	17.5	17.7	17.0	16.4	17.1	16.8	19.3	17.5	18.8
Ga	17.5	17.7	17.0	16.4	17.1	16.8	19.3	17.5	18.8
Ge	8.28	7.82	7.68	8.43	8.83	8.71	8.00	8.07	7.98
As	0.47	0.56	0.47	0.86	0.69	0.69	1.22	0.86	1.21
Se	1.384	1.50	1.54	1.38	1.418	1.5	1.423	1.56	1.41
Rb	11.4	13.1	14.5	9.11	6.6	9.55	3.45	3.87	2.79
Sr	373	358	389	439	352	475	201	300	219
Y	22.4	23.7	22.8	20.4	21.5	21.7	22.0	22.2	21.2
Zr	114.6	122.3	115	106	107	108	96.7	95.9	93.1
Nb	15.6	16.5	15.4	18.2	18.5	19.0	13.9	14.0	13.5
Mo	0.72	0.83	0.63	0.38	0.47	0.41	0.43	0.48	0.41
Ag	0.15	0.16	0.16	0.15	0.15	0.15	0.14	0.14	0.13
Cd	0.95	1.00	0.98	0.89	0.92	0.89	1.08	0.89	0.95
Sn	0.87	0.89	0.84	0.88	0.86	0.85	0.86	0.79	0.82
Sb	5.64	5.22	5.64	5.52	5.35	5.63	5.78	5.75	5.50
Cs	0.31	0.35	0.38	0.25	0.14	0.19	0.10	0.17	0.12
Ba	136	120	119	91.7	65.8	119	33.9	64.2	40.2
La	10.6	11.5	10.9	12.3	12.7	13.1	10.1	10.0	9.80
Ce	22.9	24.5	23.1	27.3	28.2	29.0	23.2	23.0	22.2
Pr	2.94	3.13	2.97	3.58	3.73	3.77	3.17	3.11	3.032
Nd	12.7	13.3	12.6	15.7	16.3	16.8	14.1	14.0	13.7
Sm	3.34	3.52	3.32	3.98	4.08	4.11	3.82	3.77	3.75
Eu	1.24	1.26	1.22	1.41	1.44	1.47	1.43	1.37	1.37
Gd	3.95	4.12	4.03	4.41	4.52	4.54	4.42	4.40	4.35
Tb	0.69	0.72	0.69	0.71	0.71	0.74	0.74	0.72	0.71
Dy	4.27	4.47	4.27	4.16	4.30	4.35	4.44	4.36	4.34
Ho	0.89	0.94	0.88	0.83	0.85	0.87	0.88	0.87	0.87

Er	2.47	2.59	2.54	2.24	2.31	2.37	2.39	2.40	2.29
Tm	0.36	0.38	0.35	0.32	0.31	0.33	0.34	0.33	0.33
Yb	2.23	2.38	2.27	1.89	1.96	1.96	2.04	2.06	1.98
Lu	0.32	0.36	0.34	0.28	0.29	0.29	0.30	0.30	0.29
Hf	2.65	2.79	2.67	2.60	2.58	2.56	2.40	2.37	2.31
Ta	1.16	1.21	1.14	1.25	1.27	1.29	0.93	0.93	0.91
W	0.15	0.17	0.15	0.10	0.15	0.14	0.08	0.09	0.08
Tl	0.06	0.08	0.07	0.07	0.07	0.08	0.04	0.04	0.04
Pb	0.86	0.94	0.92	1.54	1.33	1.43	0.81	0.82	0.81
Bi	0.01	0.02	0.02	0.01	0.01	0.01	0.01	0.01	0.01
Th	1.29	1.34	1.24	1.03	1.14	1.11	0.77	0.73	0.68
U	0.31	0.52	0.37	0.27	0.32	0.31	0.29	0.76	0.39

258

259

260

261

262

263

264

Continued Table S4

Sample	B21T76H1	B21T76H2	B21T77H1	B21T77H2	B21T77H3	B21T73H1	B21T73H2	B21T72H1	B21T72H2
Lithology	Basalt	Basalt	Basalt	Basalt	Basalt	Trachyandesite	Trachyandesite	Trachyte	Trachyte
Reference	This study								
SiO ₂	49.7	50.5	49.6	50.0	48.5	56.2	52.7	63.4	62.2
Al ₂ O ₃	17.0	16.8	16.4	16.8	15.7	16.8	16.0	18.6	18.0
Fe ₂ O ₃ T	10.2	10.5	9.99	10.1	9.62	10.1	12.7	3.07	5.42
CaO	7.38	6.58	5.29	5.13	6.34	3.14	5.23	1.47	1.48
MgO	2.79	2.82	3.47	3.26	3.24	0.26	1.02	0.54	0.33
K ₂ O	2.62	2.17	2.03	2.41	3.13	0.13	1.08	0.10	0.09
Na ₂ O	4.40	4.99	5.38	4.91	4.64	9.31	6.68	10.51	10.34
TiO ₂	2.26	2.25	1.90	2.00	1.95	1.73	2.16	0.29	0.30
P ₂ O ₅	0.78	0.78	0.69	0.69	0.73	1.01	0.87	0.08	0.09
MnO	0.20	0.21	0.20	0.19	0.18	0.05	0.07	0.05	0.05
LOI	2.26	1.90	4.72	4.38	5.47	0.76	1.36	1.69	1.53
Li	14.4	17.4	23.5	30.5	23.3	3.22	6.53	3.13	2.53
Be	2.79	2.64	2.27	1.92	1.89	2.02	3.29	1.24	1.44
B	34.7	28.7	14.0	21.0	14.1	17.3	33.6	5.73	8.28
Sc	9.27	8.72	7.30	7.41	7.47	7.87	9.18	5.98	6.01
V	93.5	95.3	69.3	72.1	72.3	43.3	97.2	11.1	18.0
Cr	10.2	8.94	19.9	19.9	29.4	8.06	4.28	5.16	5.08
Co	11.4	11.1	11.4	11.2	11.2	7.64	9.63	1.512	1.71
Ni	3.56	3.28	8.68	8.07	8.83	3.52	2.91	4.54	4.35
Cu	4.61	4.58	4.91	6.30	5.17	3.59	4.91	3.87	4.70
Zn	129	124	121	110	107	103	96.7	91.1	91.4

	21.5	20.9	22.8	23.5	20.7	11.5	17.9	16.3	14.4
Ge	8.56	8.52	7.90	9.04	8.14	7.44	10.1	3.03	4.39
As	0.81	0.72	1.71	2.97	2.48	2.48	4.60	1.35	2.13
Se	2.42	2.48	1.80	2.18	2.29	2.13	2.19	1.89	2.33
Rb	69.9	50.3	27.3	34.5	46.1	1.96	11.6	2.25	1.39
Sr	1050	1160	346	373	363	487	622.2	218	198
Y	47.1	46.7	41.0	41.2	40.1	48.2	40.5	40.4	42.5
Zr	390	385	373	363	351	385	340	1131	1279
Nb	86.8	86.0	80.8	78.1	76.0	80.4	75.4	163	178
Mo	1.28	1.18	1.56	1.70	1.42	1.36	2.12	0.80	0.98
Ag	0.39	0.40	0.35	0.37	0.38	0.37	0.33	1.09	1.19
Cd	3.07	2.91	2.66	2.83	2.81	2.76	2.62	8.01	8.89
Sn	2.10	2.20	2.15	2.17	2.04	1.62	1.94	3.42	4.65
Sb	5.43	5.63	4.24	5.14	4.76	4.00	4.45	3.97	3.36
Cs	0.31	0.24	0.11	0.46	0.09	0.08	0.11	0.04	0.07
Ba	1204	1182	377.9	607	657	50.8	284.5	16.8	20.6
La	65.1	64.3	59.3	63.0	57.6	62.6	68.1	69.0	82.2
Ce	136	133	120	129	121	133	127	162	185
Pr	16.2	15.8	14.6	15.1	14.2	16.3	15.2	19.6	21.8
Nd	63.9	62.7	57.0	59.3	55.6	64.7	60.2	68.2	77.8
Sm	12.7	12.7	11.3	11.5	10.9	12.9	12.1	11.4	13.5
Eu	4.09	4.12	3.56	3.75	3.57	4.05	3.83	2.44	3.18
Gd	12.2	12.1	10.7	10.9	10.5	12.3	11.2	9.642	11.3
Tb	1.72	1.71	1.54	1.52	1.46	1.72	1.55	1.45	1.63
Dy	9.37	9.21	8.30	8.33	7.89	9.39	8.21	7.98	8.81
Ho	1.77	1.78	1.59	1.57	1.51	1.80	1.54	1.57	1.67

Er	4.67	4.70	4.18	4.23	4.03	4.77	4.02	4.54	4.71
Tm	0.64	0.63	0.58	0.57	0.55	0.65	0.54	0.69	0.70
Yb	3.92	3.88	3.49	3.48	3.33	3.99	3.19	4.62	4.59
Lu	0.56	0.56	0.50	0.51	0.49	0.58	0.46	0.73	0.72
Hf	8.41	8.30	7.74	7.96	7.44	8.21	7.41	22.5	23.6
Ta	5.55	5.54	5.10	5.09	4.83	5.10	4.72	11.19	11.62
W	0.50	0.53	0.75	1.18	0.85	1.16	1.73	0.12	0.22
Tl	0.13	0.12	0.15	0.16	0.18	0.08	0.12	0.09	0.12
Pb	2.04	2.18	3.24	3.12	3.39	2.48	3.36	2.89	3.90
Bi	0.01	0.01	0.01	0.01	0.02	0.00	0.00	0.06	0.07
Th	5.42	5.34	4.93	5.00	4.77	5.13	4.46	11.8	12.1
U	1.29	1.28	1.03	1.20	1.06	1.27	1.04	0.96	1.05

266

267

268

269

270

271

272

Table S5. Bulk-rock major (wt.%) and trace element (ppm) data of the magmatic rocks in the Zhonggang ocean island fragment in the BNSZ

Sample	B19T84H1	B19T84H2	Oz3H1	Oz3H2	Oz3H3	Oz3H4	Oz3H5	Oz3H6	Oz3H7	Oz2H3	Oz2H2	Oz2H1	Oz4H3	Oz4H2	Oz4H1	DC13T1H3	DC13T1H4	DC13T1H5	DC13T1H6	DC13T1H7
Reference	Fan et al., 2021		Fan et al., 2014												Yu et al., 2016					
Lithology	basalt	basalt	basalt	basalt	basalt	basalt	basalt	basalt	basalt	basalt	basalt	basalt	basalt	basalt	basalt	basalt	basalt	basalt	basalt	basalt
SiO ₂	45.8	45.8	51.4	49.2	52.3	51.6	52.0	48.1	51.3	44.9	50.6	50.5	49.7	47.7	50.6	47.3	50.0	51.7	51.3	48.2
TiO ₂	2.88	2.85	3.04	2.66	2.27	2.35	2.67	4.24	2.67	2.67	2.19	1.90	2.11	3.89	3.60	4.57	4.02	3.57	4.35	4.56
Al ₂ O ₃	12.9	12.7	12.6	12.7	11.6	12.9	12.5	11.8	12.7	17.2	14.1	15.0	13.1	14.8	14.3	11.8	12.0	10.5	12.3	12.5
Fe ₂ O ₃ T	12.4	12.3	12.1	12.3	10.3	11.3	11.7	16.3	11.5	13.5	9.65	8.73	10.9	12.7	11.0	13.2	11.6	11.4	12.3	13.1
MnO	0.17	0.16	0.13	0.14	0.13	0.14	0.13	0.20	0.14	0.24	0.12	0.11	0.13	0.16	0.14	0.17	0.13	0.12	0.15	0.17
MgO	7.72	7.65	5.30	7.07	8.07	6.61	5.9	5.41	7.0	7.98	7.45	7.21	6.62	5.59	4.35	5.95	6.07	7.85	4.16	5.45
CaO	10.9	11.31	6.87	7.95	7.73	6.75	6.73	5.7	6.48	3.95	8.81	9.16	9.41	7.42	7.27	9.17	7.04	6.83	8.60	8.00
Na ₂ O	2.66	2.84	4.44	4.43	3.65	4.36	4.3	3.51	4.1	3.87	2.91	3.26	2.89	2.93	3.43	2.04	2.02	3.92	2.54	1.77
K ₂ O	1.18	0.91	1.41	1.19	1.29	1.3	1.36	2.2	1.51	0.27	0.73	0.57	0.94	1.38	2.35	1.71	4.44	0.93	1.51	2.92
P ₂ O ₅	0.37	0.4	0.35	0.29	0.27	0.29	0.31	0.51	0.28	0.43	0.21	0.19	0.25	0.34	0.36	0.47	0.63	0.50	0.57	0.47
LOI	2.99	2.97	1.40	1.39	1.27	1.09	0.97	1.13	1.04	3.94	2.45	2.51	3.27	2.23	1.67	3.23	1.89	2.05	1.61	2.49
Cr	303	361	129	298	208	239	196	19.2	240	359	309	344	336	73.3	52.6	37.1	85.8	130	15.1	20.7
Ni	107	123	72.6	118.4	72.4	97.4	83.1	52.3	94.9	161	137	168	176	55.4	43.2	46.5	62.0	86.0	34.8	42.9
Rb	59.2	33.4	15.9	12.8	14.5	15.6	16	24.5	21	9.37	13.4	9.69	17.8	22.2	34.1	38.3	113	20.1	29.8	67.8
Sr	165	168	304	474	234	303	230	435	427	335	339	255	759	480	172	1279	79.3	91.1	1036	608
Y	32.4	32.4	26.4	22.8	20.8	23.3	23.9	36.4	23.2	27.4	25.4	23.3	25.0	29.0	28.7	33.0	40.0	32.1	42.2	34.3
Zr	249	250	185	160	148	152	170	275	150	219	165	150	169	283	275	290	391	300	408	299
Nb	34.0	34.2	25.4	21.8	19.5	21.8	23.7	39.3	22.1	56.2	23.3	20.8	27.7	49.4	50.6	66.4	85.6	71.3	76.3	68.7
Cs	1.28	1.06	0.02	0.02	0.04	0.02	0.02	0.02	0.04	2.09	0.18	0.13	0.11	0.16	0.24	0.72	1.06	0.35	0.45	1.09
Ba	313	317	136	116	147	144	145	196	274	155	270	140	238	565	404	146	326	68	266	305
La	29.2	30.0	21.2	15.4	12.3	18.3	17	26.9	16.2	26.7	14.4	13.8	17.4	29.7	30.1	35.0	45.5	38.3	42.3	36.8
Ce	64.9	66.7	46.2	35.3	30.2	40	39.9	62.5	36.9	58.0	34.5	32.6	39.4	65.9	66.8	79.0	110	84.6	104	82.7

Pr	7.92	8.08	5.96	4.69	4.15	5.21	5.27	8.25	4.86	7.60	4.86	4.59	5.34	8.77	8.77	10.0	12.9	10.5	12.6	10.5
Nd	36.0	36.7	26.4	21.1	19	23.1	23.5	36.7	21.8	32.1	22.2	21.0	23.6	38.0	37.9	45.2	57.7	46.4	57.7	47.2
Sm	8.37	8.47	6.19	5.13	4.7	5.47	5.5	8.63	5.24	7.07	5.60	5.27	5.64	8.58	8.48	10.1	12.4	10.1	13.1	10.6
Eu	2.65	2.61	2.05	1.74	1.48	1.86	1.79	2.57	1.78	2.31	1.74	1.76	1.95	2.92	2.72	3.23	3.89	3.15	4.18	3.41
Gd	7.92	8.03	6.3	5.24	4.81	5.59	5.6	8.66	5.4	6.78	5.84	5.50	5.82	8.30	8.07	9.82	11.7	9.62	12.6	10.3
Tb	1.16	1.17	0.94	0.8	0.73	0.83	0.84	1.29	0.81	0.96	0.87	0.82	0.85	1.15	1.11	1.34	1.59	1.29	1.71	1.39
Dy	6.81	6.93	5.33	4.59	4.17	4.73	4.83	7.36	4.64	5.51	5.11	4.79	4.98	6.28	6.11	7.46	8.92	7.26	9.52	7.78
Ho	1.26	1.27	0.99	0.85	0.77	0.87	0.9	1.36	0.86	1.02	0.94	0.88	0.93	1.10	1.07	1.30	1.58	1.26	1.66	1.36
Er	3.23	3.24	2.61	2.26	2.04	2.31	2.38	3.63	2.27	2.78	2.55	2.38	2.53	2.80	2.75	3.43	4.22	3.35	4.32	3.58
Tm	0.42	0.43	0.34	0.3	0.27	0.3	0.31	0.48	0.3	0.36	0.32	0.31	0.32	0.35	0.33	0.42	0.53	0.42	0.54	0.44
Yb	2.49	2.52	2.08	1.79	1.61	1.83	1.91	2.93	1.81	2.25	1.99	1.89	1.99	2.07	2.01	2.55	3.24	2.53	3.28	2.68
Lu	0.36	0.36	0.29	0.25	0.22	0.25	0.27	0.41	0.25	0.31	0.28	0.26	0.28	0.28	0.27	0.34	0.43	0.33	0.43	0.36
Hf	6.40	6.46	4.47	3.83	3.55	3.9	4.16	6.8	3.87	5.10	4.09	3.86	4.18	6.53	6.37	7.31	9.47	7.28	10.16	7.61
Ta	2.27	2.31	1.5	1.28	1.13	1.27	1.36	2.23	1.28	3.44	1.50	1.44	3.09	3.19	3.49	4.32	6.08	4.76	5.02	4.58
Pb	1.83	1.87	1.52	1.31	1.03	1.25	1.24	4.35	4.83	2.23	0.80	0.71	1.37	1.80	1.82	2.65	2.33	2.20	3.21	2.80
Th	3.99	4.01	2.13	1.95	1.72	1.95	2.06	3.29	1.92	3.10	1.36	1.32	1.75	3.06	3.18	4.28	5.93	5.05	5.35	4.56
U	1.03	1.04	0.48	0.42	0.37	0.42	0.44	0.74	0.43	0.81	0.43	0.39	0.36	0.95	0.90	1.07	1.54	1.18	1.33	1.14

274

275

Continued Table S5

Sample	DC13T1H10	DC13T1H11	DC13T1H14	11DC-23	11DC-25	11DC-26	11DC-27	11DC-28	11DC-30	11DC-40	11DC-41	11DC-42	11DC-43	11DC-44	D18T22H1	D18T22H2	DC13T1H8	DC13T1H9
Reference	Yu et al., 2016				Wang et al., 2016								Fan et al., 2021			Yu et al., 2015		
Lithology	basalt	basalt	basalt	basalt	basalt	basalt	basalt	basalt	basalt	basalt	basalt	basalt	basalt	Trachyandesite	Trachyandesite	Trachyandesite	Trachyandesite	
SiO ₂	52.1	48.0	51.9	47.5	45.8	45.4	46.2	46.1	45.9	52.5	45.7	47.5	46.2	47.7	53.2	53.8	54.0	55.4
TiO ₂	2.67	4.30	2.12	3.06	3.31	3.42	3.55	3.40	3.63	2.38	3.25	3.02	3.58	2.98	1.78	1.82	2.00	2.21
Al ₂ O ₃	9.9	11.7	15.0	12.8	15.9	15.7	16.7	16.1	14.8	11.2	12.7	12.3	13.2	12.3	16.6	16.5	17.3	15.5
Fe ₂ O ₃ T	9.75	14.0	10.0	13.1	12.8	13.1	12.7	12.9	12.3	10.2	13.1	12.2	12.9	11.9	10.6	10.7	6.78	8.82
MnO	0.12	0.19	0.13	0.16	0.18	0.20	0.21	0.21	0.15	0.12	0.16	0.18	0.18	0.16	0.12	0.10	0.13	0.12
MgO	6.23	5.90	3.29	7.58	5.42	5.44	4.66	4.44	5.67	7.32	8.56	8.12	6.91	8.12	1.73	1.58	2.01	2.46
CaO	10.58	8.63	8.34	7.60	6.67	7.90	6.89	5.98	8.76	8.88	8.28	8.87	7.97	8.76	3.61	3.64	7.01	5.74
Na ₂ O	2.27	2.17	3.97	3.81	3.70	4.07	4.69	4.28	4.40	3.95	2.51	3.29	1.58	3.72	8.21	8.37	6.06	5.26
K ₂ O	2.30	2.60	0.55	0.50	1.58	0.38	1.15	2.60	0.13	1.64	1.84	1.27	4.02	1.01	0.52	0.47	0.76	1.39
P ₂ O ₅	0.26	0.52	0.76	0.29	0.41	0.39	0.37	0.84	0.33	0.15	0.21	0.26	0.32	0.24	1.23	1.24	0.65	0.71
LOI	3.36	1.61	3.18	3.54	3.47	3.82	2.77	3.12	3.76	1.59	3.50	2.98	3.08	3.04	2.23	1.81	2.56	1.67
Cr	487	36.3	2.22	100	36	38	31	23	40	297	272	327	114	232	11.5	4.56	58.3	20.3
Ni	219	63.7	4.34	54.4	31.2	33.4	10.4	15.2	38.5	147	139	148	70.9	121	80.6	74.9	18.4	15.0
Rb	49.4	57.6	9.95	8.18	61.4	10.2	29.4	57.6	1.3	44.5	23.1	15.6	39.4	14.2	2.88	1.50	15.0	37.0
Sr	397	392	271	191	355	403	571	417	221	81.5	181	155	258	154	285	299	705	490
Y	24.5	36.4	25.5	29.4	30.8	31.1	30.9	36.6	32.0	24.1	28.3	27.6	31.9	26.5	45.5	50.2	38.3	43.3
Zr	197	331	244	226	330	336	299	408	312	161	221	209	244	201	1056	1060	417	478
Nb	34.4	70.4	91.0	23.9	58.9	60.1	66.9	91.6	48.1	14.7	30.5	28.6	34.2	28.0	151	151	98	101
Cs	0.57	0.67	0.75	0.69	0.68	0.50	2.16	2.92	0.23	0.42	0.35	0.33	0.26	0.32	0.13	0.10	3.85	0.74
Ba	442	282	132	295	396	324	824	778	133	72.0	392	344	852	294	54.0	51.7	501	322
La	21.7	39.7	45.0	23.4	34.3	34.4	37.2	59.3	30.7	12.3	19.2	19.8	24.0	18.9	38.4	47.0	57.3	59.7
Ce	50.7	93.7	93.9	53.4	71.8	72.6	77.9	122	68.6	30.4	45.1	45.6	54.3	43.9	96.9	115	135	147

Pr	6.59	11.5	10.7	7.66	9.54	9.70	10.2	15.7	9.60	4.53	6.59	6.60	7.77	6.39	15.3	18.5	15.3	16.9
Nd	30.0	51.7	44.4	33.4	39.2	39.7	41.4	62.4	41.2	20.8	29.7	29.7	34.5	28.2	65.9	78.8	65.4	73.5
Sm	6.90	11.3	8.99	7.55	8.04	8.03	8.43	11.6	8.69	4.98	6.99	6.85	7.98	6.75	15.8	18.0	13.0	15.1
Eu	2.27	3.58	2.90	2.38	2.59	2.59	2.59	3.52	2.68	1.63	2.21	2.26	2.57	2.14	5.01	5.71	4.89	5.04
Gd	6.814	10.8	8.18	7.63	7.73	7.71	8.04	10.2	8.33	5.20	7.04	6.97	7.99	6.77	14.6	16.3	11.7	13.7
Tb	0.96	1.47	1.07	1.11	1.13	1.14	1.15	1.45	1.21	0.83	1.06	1.05	1.19	1.00	2.26	2.43	1.55	1.81
Dy	5.40	8.16	5.80	6.15	6.06	6.25	6.37	7.64	6.55	4.74	5.81	5.82	6.61	5.60	12.0	12.8	8.48	9.89
Ho	0.96	1.42	0.98	1.18	1.16	1.19	1.25	1.43	1.26	0.93	1.13	1.13	1.28	1.10	2.32	2.40	1.49	1.69
Er	2.54	3.75	2.49	2.92	2.95	3.09	3.05	3.57	3.09	2.32	2.75	2.75	3.05	2.69	6.11	6.34	3.95	4.45
Tm	0.32	0.46	0.30	0.39	0.42	0.41	0.41	0.48	0.41	0.32	0.36	0.37	0.40	0.34	0.87	0.87	0.50	0.55
Yb	1.96	2.79	1.78	2.26	2.58	2.64	2.60	2.93	2.48	1.87	2.22	2.14	2.37	2.13	4.91	5.03	3.01	3.39
Lu	0.26	0.36	0.23	0.34	0.38	0.40	0.38	0.42	0.36	0.27	0.31	0.30	0.36	0.30	0.77	0.76	0.41	0.45
Hf	5.08	8.29	4.53	5.46	7.13	7.38	6.58	8.61	7.02	3.89	5.35	5.13	5.82	4.96	22.6	23.5	9.16	11.0
Ta	2.28	4.58	5.45	1.20	3.65	3.76	3.91	5.01	2.99	0.62	1.94	1.83	2.10	1.79	9.93	9.60	6.03	6.34
Pb	1.82	2.04	1.94	1.67	2.55	4.26	4.27	6.64	1.87	1.90	1.39	1.19	1.84	2.10	4.63	4.29	1.63	2.64
Th	2.50	4.84	6.00	2.94	4.74	4.81	5.70	8.36	4.03	1.71	2.60	2.48	3.02	2.42	4.62	5.19	6.80	7.36
U	0.75	1.23	1.59	0.85	1.30	1.32	1.45	2.05	1.18	0.57	0.79	0.70	0.82	0.69	1.36	1.46	3.75	1.70

277

References cited

- Fan, J.J., Li, C., Xie, C.M., and Wang, M., 2014. Petrology, geochemistry, and geochronology of the Zhonggang ocean island, northern Tiber: implications for the evolution of the Bangongco–Nujiang oceanic arm of Neo-Tethys: International Geology Review, v. 56, p. 1504–1520.
- Fan, J.J., Niu, Y.L., Liu, Y.M., Hao, Y.J., 2021. Timing of closure of the Meso-Tethys Ocean: Constraints from remnants of a 141–135 Ma ocean island within the Bangong–Nujiang Suture Zone, Tibetan Plateau. Geological Society of America Bulletin, v. 133, p.1875–1889.
- Wang, B.D., Wang, L.Q., Chung, S.L., Chen, J.L., Yin, F.G., Liu, H., Li, X.B., and Chen, L.X., 2016. Evolution of the Bangong–Nujiang Tethyan ocean: Insights from the geochronology and geochemistry of mafic rocks within ophiolites: Lithos, v. 245, p. 18–33.
- Yu, Y.P., Hu, P.Y., Li, C., Xie, C.M., Fan, J.J., Xu, W., and Liu, J.H., 2016. The Petrology and geochemistry of Early Cretaceous ocean island volcanic rocks in the middle-western segment of Bangong Co-Nujiang suture zone: Geological Bulletin of China, v. 35, p. 1281-1290 (in Chinese with English abstract).

285

Table S6 Zircon LA-ICP-MS U-Pb data of the magmatic rocks in the Nare intraplate ocean island fragment in the BNSZ

Spots	Th	U	Th/U	isotope ratio ($\pm 1\sigma$) (measured ratios)				isotope ratio ($\pm 1\sigma$) (corrected ratios)				age (Ma $\pm 1\sigma$)				Discordance						
				$^{207}\text{Pb}/^{206}\text{Pb}$		$^{207}\text{Pb}/^{235}\text{U}$		$^{206}\text{Pb}/^{238}\text{U}$		$^{207}\text{Pb}/^{206}\text{Pb}$		$^{207}\text{Pb}/^{235}\text{U}$		$^{206}\text{Pb}/^{238}\text{U}$		$^{207}\text{Pb}/^{206}\text{Pb}$						
				ratios	1σ	ratios	1σ	ratios	1σ	ratios	1σ	ratios	1σ	age	ratio	age	1σ					
B21T65-01	657	568	1.16	0.0512	0.00272	0.27749	0.01458	0.03932	0.00105	0.0512	0.00272	0.27749	0.01458	0.03932	0.00105	250	73	249	12	249	7	0.00%
B21T65-02	108	147	0.74	0.05115	0.00457	0.26703	0.02322	0.03788	0.00126	0.05115	0.00457	0.26703	0.02322	0.03788	0.00126	248	136	240	19	240	8	0.00%
B21T65-03	311	295	1.05	0.05091	0.00467	0.26938	0.02411	0.0384	0.00127	0.05091	0.00467	0.26938	0.02411	0.0384	0.00127	237	142	242	19	243	8	-0.41%
B21T65-04	336	309	1.09	0.05102	0.00364	0.2765	0.01951	0.03932	0.00111	0.05102	0.00364	0.2765	0.01951	0.03932	0.00111	242	111	248	16	249	7	-0.40%
B21T65-05	396	343	1.15	0.05089	0.00355	0.2647	0.01807	0.03774	0.00111	0.05089	0.00355	0.2647	0.01807	0.03774	0.00111	236	103	238	15	239	7	-0.42%
B21T65-06	248	213	1.16	0.05119	0.00394	0.27444	0.02074	0.03891	0.00116	0.05119	0.00394	0.27444	0.02074	0.03891	0.00116	249	118	246	17	246	7	0.00%
B21T65-07	655	576	1.14	0.05137	0.00271	0.27206	0.01422	0.03843	0.00103	0.05137	0.00271	0.27206	0.01422	0.03843	0.00103	257	72	244	11	243	6	0.41%
B21T65-08	210	223	0.94	0.05056	0.00312	0.27538	0.01671	0.03952	0.00111	0.05056	0.00312	0.27538	0.01671	0.03952	0.00111	221	89	247	13	250	7	-1.20%
B21T65-09	425	442	0.88	0.05604	0.00654	0.28652	0.03234	0.0374	0.0015	0.05604	0.00654	0.28652	0.03234	0.0374	0.0015	454	180	256	26	235	9	8.94%
B21T65-10	762	618	1.23	0.05107	0.00246	0.28371	0.01363	0.04031	0.00106	0.05107	0.00246	0.28371	0.01363	0.04031	0.00106	244	64	254	11	255	7	-0.39%
B21T65-11	604	579	1.04	0.0525	0.00363	0.28747	0.01981	0.03974	0.00106	0.0525	0.00363	0.28747	0.01981	0.03974	0.00106	307	108	257	16	251	7	2.39%
B21T65-12	398	358	1.11	0.05084	0.00315	0.2669	0.0163	0.0381	0.00108	0.05084	0.00315	0.2669	0.0163	0.0381	0.00108	234	89	240	13	241	7	-0.41%
B21T65-13	1125	630	1.79	0.05086	0.00251	0.2753	0.01354	0.03928	0.00104	0.05086	0.00251	0.2753	0.01354	0.03928	0.00104	234	66	247	11	248	6	-0.40%
B21T65-14	1318	920	1.43	0.05125	0.00182	0.28016	0.01021	0.03968	0.00098	0.05125	0.00182	0.28016	0.01021	0.03968	0.00098	252	42	251	8	251	6	0.00%
B21T65-15	159	163	0.98	0.05114	0.0041	0.28275	0.0222	0.04013	0.00125	0.05114	0.0041	0.28275	0.0222	0.04013	0.00125	247	122	253	18	254	8	-0.39%
B21T65-16	605	586	1.03	0.05105	0.00233	0.27422	0.01256	0.03898	0.00101	0.05105	0.00233	0.27422	0.01256	0.03898	0.00101	243	59	246	10	247	6	-0.40%
B21T65-17	867	599	1.45	0.04839	0.00244	0.26077	0.0131	0.03911	0.00104	0.04839	0.00244	0.26077	0.0131	0.03911	0.00104	448	68	235	11	247	6	-4.86%
B21T65-18	395	353	1.12	0.05116	0.00319	0.27749	0.01719	0.03937	0.00109	0.05116	0.00319	0.27749	0.01719	0.03937	0.00109	248	92	249	14	249	7	0.00%
B21T65-19	78	105	0.74	0.05121	0.01091	0.26992	0.05695	0.03826	0.00155	0.05121	0.01091	0.26992	0.05695	0.03826	0.00155	250	343	243	46	242	10	0.41%
B21T65-20	345	330	1.05	0.05099	0.00372	0.27427	0.01986	0.03905	0.0011	0.05099	0.00372	0.27427	0.01986	0.03905	0.0011	240	114	246	16	247	7	-0.40%
B21T65-21	2146	1044	2.06	0.05043	0.00178	0.27226	0.0099	0.03919	0.00098	0.05043	0.00178	0.27226	0.0099	0.03919	0.00098	215	42	244	8	248	6	-1.61%

B21T65-22	610	466	1.31	0.05097	0.00264	0.27402	0.01419	0.03903	0.00105	0.05097	0.00264	0.27402	0.01419	0.03903	0.00105	239	71	246	11	247	7	-0.40%
B21T65-23	927	626	1.48	0.05098	0.00259	0.2752	0.01394	0.03919	0.00106	0.05098	0.00259	0.2752	0.01394	0.03919	0.00106	240	68	247	11	248	7	-0.40%
B21T64-01	221	233	0.95	0.05106	0.00463	0.27496	0.02443	0.03906	0.00125	0.05106	0.00463	0.27496	0.02443	0.03906	0.00125	244	143	247	19	247	8	0.00%
B21T64-02	910	504	1.81	0.05163	0.00496	0.27439	0.02617	0.03855	0.00109	0.05163	0.00496	0.27439	0.02617	0.03855	0.00109	269	164	246	21	244	7	0.82%
B21T64-03	685	397	1.73	0.05087	0.00433	0.27166	0.02302	0.03873	0.00104	0.05087	0.00433	0.27166	0.02302	0.03873	0.00104	235	143	244	18	245	6	-0.41%
B21T64-04	64	145	0.44	0.05129	0.00617	0.28254	0.03368	0.03995	0.0012	0.05129	0.00617	0.28254	0.03368	0.03995	0.0012	254	213	253	27	253	7	0.00%
B21T64-05	1903	777	2.45	0.05141	0.00306	0.27525	0.01635	0.03883	0.00099	0.05141	0.00306	0.27525	0.01635	0.03883	0.00099	259	90	247	13	246	6	0.41%
B21T64-06	240	251	0.95	0.05122	0.00574	0.27875	0.03102	0.03947	0.00114	0.05122	0.00574	0.27875	0.03102	0.03947	0.00114	251	197	250	25	250	7	0.00%
B21T64-07	876	447	1.96	0.05006	0.00303	0.26534	0.01574	0.03844	0.00107	0.05006	0.00303	0.26534	0.01574	0.03844	0.00107	198	87	239	13	243	7	-1.65%
B21T61-01	227	255	0.89	0.051	0.00503	0.27107	0.0263	0.03855	0.00128	0.051	0.00503	0.27107	0.0263	0.03855	0.00128	241	158	244	21	244	8	0.00%
B21T61-02	142	166	0.86	0.05096	0.00601	0.26369	0.03041	0.03754	0.00141	0.05096	0.00601	0.26369	0.03041	0.03754	0.00141	239	190	238	24	238	9	0.00%
B21T61-03	177	190	0.93	0.0509	0.00586	0.26591	0.02992	0.0379	0.00142	0.0509	0.00586	0.26591	0.02992	0.0379	0.00142	236	184	239	24	240	9	-0.42%
B21T61-04	194	232	0.83	0.04919	0.00421	0.26847	0.02255	0.03959	0.00127	0.04919	0.00421	0.26847	0.02255	0.03959	0.00127	157	130	241	48	250	8	-3.60%
B21T61-05	177	188	0.94	0.05093	0.00597	0.26932	0.03115	0.03836	0.00129	0.05093	0.00597	0.26932	0.03115	0.03836	0.00129	238	198	242	25	243	8	-0.41%
B21T61-06	183	192	0.95	0.0513	0.00867	0.26703	0.0448	0.03776	0.0013	0.0513	0.00867	0.26703	0.0448	0.03776	0.0013	254	294	240	36	239	8	0.42%
B21T61-07	214	245	0.87	0.05174	0.00794	0.27257	0.04164	0.03822	0.0012	0.05174	0.00794	0.27257	0.04164	0.03822	0.0012	274	283	245	33	242	7	1.24%
B21T61-08	204	212	0.96	0.05079	0.00362	0.276	0.01942	0.03942	0.00117	0.05079	0.00362	0.276	0.01942	0.03942	0.00117	231	107	247	15	249	7	-0.80%
B21T61-09	393	359	1.09	0.05187	0.0049	0.27192	0.02559	0.03803	0.00109	0.05187	0.0049	0.27192	0.02559	0.03803	0.00109	280	160	244	20	241	7	1.24%
B21T61-10	146	172	0.85	0.05099	0.00836	0.26526	0.04307	0.03773	0.00135	0.05099	0.00836	0.26526	0.04307	0.03773	0.00135	240	283	239	35	239	8	0.00%

287

288

289

290

Table S7 Zircon LA-ICP-MS U-Pb data of the magmatic rocks in the Maqiao intraplate ocean island fragment in the BNSZ

Spots	Th	U	Th/U	isotope ratio ($\pm 1\sigma$) (measured ratios)				isotope ratio ($\pm 1\sigma$) (corrected ratios)				age (Ma $\pm 1\sigma$)				Discordance						
				$^{207}\text{Pb}/^{206}\text{Pb}$		$^{207}\text{Pb}/^{235}\text{U}$		$^{206}\text{Pb}/^{238}\text{U}$		$^{207}\text{Pb}/^{206}\text{Pb}$		$^{207}\text{Pb}/^{235}\text{U}$		$^{206}\text{Pb}/^{238}\text{U}$		$^{207}\text{Pb}/^{206}\text{Pb}$						
				ratios	1σ	ratios	1σ	ratios	1σ	ratios	1σ	ratios	1σ	age	ratio	age	1σ	age	1σ			
ShT42-01	364	364	4	0.05142	0.00185	0.22551	0.00876	0.0318	0.00083	0.05142	0.00185	0.22551	0.00876	0.0318	0.00083	260	45	206	7	202	5	+0.98%
ShT42-02	171	229	0.74	0.05036	0.0018	0.22804	0.00877	0.03284	0.00087	0.05036	0.0018	0.22804	0.00877	0.03284	0.00087	212	44	209	7	208	5	0.48%
ShT42-03	337	399	0.84	0.05111	0.00177	0.23455	0.00883	0.03328	0.00087	0.05111	0.00177	0.23455	0.00883	0.03328	0.00087	246	43	214	7	211	5	1.42%
ShT42-04	41	111	0.37	0.05021	0.00284	0.22561	0.01304	0.03259	0.0009	0.05021	0.00284	0.22561	0.01304	0.03259	0.0009	205	83	207	11	207	6	0.00%
ShT42-05	9	34	0.26	0.0485	0.00975	0.21546	0.04324	0.03222	0.00107	0.0485	0.00975	0.21546	0.04324	0.03222	0.00107	124	316	198	36	204	7	-2.94%
ShT42-06	50	106	0.47	0.04935	0.00324	0.22596	0.0151	0.03321	0.00091	0.04935	0.00324	0.22596	0.0151	0.03321	0.00091	164	102	207	13	211	6	-1.90%
ShT42-07	200	239	0.84	0.0503	0.00177	0.22979	0.00873	0.03313	0.00087	0.0503	0.00177	0.22979	0.00873	0.03313	0.00087	209	44	210	7	210	5	0.00%
ShT42-08	841	705	1.19	0.0502	0.0013	0.22656	0.0068	0.03273	0.00084	0.0502	0.0013	0.22656	0.0068	0.03273	0.00084	204	31	207	6	208	5	-0.48%
ShT42-09	85	126	0.68	0.04955	0.00305	0.22357	0.01402	0.03272	0.00089	0.04955	0.00305	0.22357	0.01402	0.03272	0.00089	174	94	205	12	208	6	-1.44%
ShT42-10	64	121	0.53	0.05025	0.00298	0.22677	0.01365	0.03273	0.00092	0.05025	0.00298	0.22677	0.01365	0.03273	0.00092	207	88	208	11	208	6	0.00%
ShT42-11	400	402	0.99	0.05049	0.0016	0.22999	0.00805	0.03303	0.00086	0.05049	0.0016	0.22999	0.00805	0.03303	0.00086	218	38	210	7	209	5	0.48%
ShT42-12	86	127	0.67	0.05036	0.00256	0.22512	0.01175	0.03242	0.00089	0.05036	0.00256	0.22512	0.01175	0.03242	0.00089	212	71	206	10	206	6	0.00%
ShT42-13	1713	789	2.17	0.05051	0.00126	0.22473	0.00658	0.03226	0.00083	0.05051	0.00126	0.22473	0.00658	0.03226	0.00083	219	30	206	5	205	5	0.49%
ShT42-14	51	83	0.62	0.05	0.00268	0.21856	0.01184	0.0317	0.00092	0.05	0.00268	0.21856	0.01184	0.0317	0.00092	195	73	201	10	201	6	0.00%
ShT42-15	102	137	0.75	0.05032	0.0024	0.22545	0.01112	0.03249	0.00088	0.05032	0.0024	0.22545	0.01112	0.03249	0.00088	210	65	206	9	206	5	0.00%
ShT42-16	77	86	0.89	0.05017	0.00255	0.22496	0.0118	0.03252	0.00088	0.05017	0.00255	0.22496	0.0118	0.03252	0.00088	203	72	206	10	206	5	0.00%
ShT42-17	17	39	0.43	0.05065	0.00718	0.22891	0.0324	0.03277	0.00103	0.05065	0.00718	0.22891	0.0324	0.03277	0.00103	225	257	209	27	208	6	0.48%
ShT42-18	55	116	0.47	0.05017	0.00326	0.22922	0.01518	0.03313	0.0009	0.05017	0.00326	0.22922	0.01518	0.03313	0.0009	203	103	210	13	210	6	0.00%
ShT42-19	32	61	0.52	0.05022	0.00456	0.22333	0.02037	0.03225	0.00092	0.05022	0.00456	0.22333	0.02037	0.03225	0.00092	205	152	205	17	205	6	0.00%
ShT42-20	406	473	0.86	0.05016	0.00148	0.22073	0.00728	0.03191	0.00082	0.05016	0.00148	0.22073	0.00728	0.03191	0.00082	202	35	203	6	202	5	0.50%
B19T38-01	20	75	0.27	0.04998	0.00459	0.21729	0.01952	0.03152	0.00105	0.04998	0.00459	0.21729	0.01952	0.03152	0.00105	194	141	200	16	200	7	0.00%

B19T38-02	101	146	0.7	0.05004	0.00431	0.21853	0.01854	0.03166	0.001	0.05004	0.00431	0.21853	0.01854	0.03166	0.001	197	134	201	15	201	6	0.00%
B19T38-03	31	59	0.53	0.05013	0.00485	0.22222	0.02094	0.03214	0.00114	0.05013	0.00485	0.22222	0.02094	0.03214	0.00114	201	147	204	17	204	7	0.00%
B19T38-04	49	132	0.38	0.05044	0.0044	0.21782	0.01872	0.03131	0.00098	0.05044	0.0044	0.21782	0.01872	0.03131	0.00098	215	137	200	16	199	6	0.50%
B19T38-05	330	326	1.01	0.04954	0.00231	0.22622	0.01066	0.03311	0.00089	0.04954	0.00231	0.22622	0.01066	0.03311	0.00089	173	62	207	9	210	6	-1.43%
B19T38-06	357	325	1.1	0.05083	0.00324	0.23096	0.01481	0.03295	0.00088	0.05083	0.00324	0.23096	0.01481	0.03295	0.00088	233	98	211	12	209	5	0.96%
B19T38-07	47	70	0.67	0.05003	0.00496	0.21645	0.02091	0.03137	0.00113	0.05003	0.00496	0.21645	0.02091	0.03137	0.00113	196	151	199	17	199	7	0.00%
B19T38-08	53	77	0.69	0.05003	0.00693	0.22407	0.03069	0.03248	0.00113	0.05003	0.00693	0.22407	0.03069	0.03248	0.00113	196	240	205	25	206	7	-0.49%
B19T38-09	18	44	0.4	0.05031	0.00542	0.22809	0.02392	0.03287	0.00125	0.05031	0.00542	0.22809	0.02392	0.03287	0.00125	209	166	209	20	208	8	0.48%
B19T38-10	154	254	0.61	0.04928	0.00242	0.21932	0.01088	0.03227	0.00088	0.04928	0.00242	0.21932	0.01088	0.03227	0.00088	161	66	201	9	205	5	-1.95%
B19T38-11	264	264	4	0.04829	0.00287	0.21391	0.01264	0.03212	0.00093	0.04829	0.00287	0.21391	0.01264	0.03212	0.00093	114	82	197	14	204	6	-3.43%
B19T38-12	31	62	0.5	0.04876	0.00496	0.21991	0.02144	0.0327	0.00134	0.04876	0.00496	0.21991	0.02144	0.0327	0.00134	136	143	202	18	207	8	-2.42%
B19T38-13	368	354	1.04	0.05013	0.00261	0.2271	0.012	0.03285	0.00088	0.05013	0.00261	0.2271	0.012	0.03285	0.00088	201	74	208	10	208	5	0.00%
B19T38-14	83	140	0.59	0.0511	0.0035	0.22151	0.01493	0.03143	0.00098	0.0511	0.0035	0.22151	0.01493	0.03143	0.00098	245	98	203	12	199	6	2.01%
B19T38-15	44	66	0.67	0.05027	0.00787	0.22195	0.03455	0.03202	0.00107	0.05027	0.00787	0.22195	0.03455	0.03202	0.00107	207	272	204	29	203	7	0.49%
B19T38-16	47	117	0.4	0.05007	0.0038	0.21843	0.01632	0.03164	0.00101	0.05007	0.0038	0.21843	0.01632	0.03164	0.00101	198	112	201	14	201	6	0.00%
B19T38-17	9	29	0.3	0.05034	0.01469	0.21841	0.06314	0.03146	0.00156	0.05034	0.01469	0.21841	0.06314	0.03146	0.00156	211	435	201	53	200	10	0.50%
B19T38-18	192	233	0.83	0.05141	0.00406	0.2328	0.01851	0.03284	0.0009	0.05141	0.00406	0.2328	0.01851	0.03284	0.0009	259	131	213	15	208	6	2.40%

292

293

294

295

296

Table S8 Zircon LA-ICP-MS U-Pb data of the magmatic rocks in the Tarenben intraplate ocean island fragment in the BNSZ

Spots	Th	U	Th/U	isotope ratio ($\pm 1\sigma$) (measured ratios)				isotope ratio ($\pm 1\sigma$) (corrected ratios)				age (Ma $\pm 1\sigma$)				Discordance						
				$^{207}\text{Pb}/^{206}\text{Pb}$		$^{207}\text{Pb}/^{235}\text{U}$		$^{206}\text{Pb}/^{238}\text{U}$		$^{207}\text{Pb}/^{206}\text{Pb}$		$^{207}\text{Pb}/^{235}\text{U}$		$^{206}\text{Pb}/^{238}\text{U}$		$^{207}\text{Pb}/^{206}\text{Pb}$						
				ratios	1σ	ratios	1σ	ratios	1σ	ratios	1σ	ratios	1σ	age	ratio	age	1σ	age	1σ			
B21T72-01	135	186	0.72	0.05014	0.0152	0.23579	0.07115	0.03409	0.00139	0.05014	0.0152	0.23579	0.07115	0.03409	0.00139	201	470	215	58	216	9	-0.46%
B21T72-02	180	217	0.83	0.05102	0.01438	0.22844	0.06402	0.03246	0.00131	0.05102	0.01438	0.22844	0.06402	0.03246	0.00131	242	444	209	53	206	8	1.46%
B21T72-03	114	190	0.6	0.05015	0.0079	0.23651	0.03657	0.03419	0.00141	0.05015	0.0079	0.23651	0.03657	0.03419	0.00141	202	265	216	30	217	9	-0.46%
B21T72-04	109	146	0.74	0.05022	0.01255	0.22972	0.0568	0.03316	0.0015	0.05022	0.01255	0.22972	0.0568	0.03316	0.0015	205	381	210	47	210	9	0.00%
B21T72-05	120	145	0.83	0.04944	0.01049	0.23214	0.04824	0.03404	0.00176	0.04944	0.01049	0.23214	0.04824	0.03404	0.00176	169	311	212	40	216	11	-1.85%
B21T72-06	144	205	0.7	0.05025	0.0083	0.22719	0.0368	0.03278	0.00139	0.05025	0.0083	0.22719	0.0368	0.03278	0.00139	207	273	208	30	208	9	0.00%
B21T72-07	134	183	0.73	0.05026	0.00941	0.22544	0.04157	0.03252	0.00138	0.05026	0.00941	0.22544	0.04157	0.03252	0.00138	207	302	206	34	206	9	0.00%
B21T72-08	342	282	1.21	0.05039	0.01321	0.23124	0.06034	0.03327	0.00122	0.05039	0.01321	0.23124	0.06034	0.03327	0.00122	213	414	211	50	211	8	0.00%
B21T72-09	200	248	0.81	0.05039	0.00702	0.23363	0.03196	0.03362	0.00128	0.05039	0.00702	0.23363	0.03196	0.03362	0.00128	213	237	213	26	213	8	0.00%
B21T72-10	193	239	0.81	0.05026	0.00732	0.22033	0.03122	0.03179	0.00137	0.05026	0.00732	0.22033	0.03122	0.03179	0.00137	207	235	202	26	202	9	0.00%
B21T72-11	314	265	1.18	0.04972	0.01165	0.22371	0.05208	0.03262	0.00121	0.04972	0.01165	0.22371	0.05208	0.03262	0.00121	182	371	205	43	207	8	-0.97%
B21T72-12	220	252	0.87	0.05045	0.00734	0.23304	0.03332	0.03349	0.00127	0.05045	0.00734	0.23304	0.03332	0.03349	0.00127	216	248	213	27	212	8	0.47%
B21T72-13	98	144	0.68	0.05026	0.0113	0.22848	0.0506	0.03296	0.00156	0.05026	0.0113	0.22848	0.0506	0.03296	0.00156	207	341	209	42	209	10	0.00%
B21T72-14	231	237	0.97	0.04499	0.00643	0.20814	0.02903	0.03355	0.00137	0.04499	0.00643	0.20814	0.02903	0.03355	0.00137	-29	203	192	24	213	9	-9.86%
B21T72-15	86	143	0.6	0.05055	0.01703	0.23087	0.07722	0.03312	0.00161	0.05055	0.01703	0.23087	0.07722	0.03312	0.00161	220	506	211	64	210	10	0.48%
B21T72-16	83	174	0.48	0.04965	0.0075	0.23249	0.03442	0.03396	0.00137	0.04965	0.0075	0.23249	0.03442	0.03396	0.00137	179	251	212	28	215	9	-1.40%
B21T72-17	194	210	0.92	0.04897	0.00708	0.22994	0.03256	0.03405	0.00133	0.04897	0.00708	0.22994	0.03256	0.03405	0.00133	146	242	210	27	216	8	-2.78%
B21T72-18	40	77	0.53	0.05027	0.0167	0.23099	0.07579	0.03332	0.00196	0.05027	0.0167	0.23099	0.07579	0.03332	0.00196	207	484	211	63	211	12	0.00%
B21T72-19	66	151	0.44	0.05006	0.0087	0.22647	0.03852	0.03281	0.00146	0.05006	0.0087	0.22647	0.03852	0.03281	0.00146	198	280	207	32	208	9	-0.48%
B21T72-20	479	340	1.41	0.0502	0.00593	0.22576	0.02611	0.03261	0.00112	0.0502	0.00593	0.22576	0.02611	0.03261	0.00112	204	196	207	22	207	7	0.00%
B21T72-21	101	159	0.63	0.04978	0.01766	0.22922	0.08091	0.03339	0.00145	0.04978	0.01766	0.22922	0.08091	0.03339	0.00145	185	537	210	67	212	9	-0.94%

B21T72-22	110	159	0.69	0.04905	0.00812	0.22768	0.03688	0.03366	0.00144	0.04905	0.00812	0.22768	0.03688	0.03366	0.00144	150	265	208	31	213	9	-2.35%
B21T72-23	110	164	0.67	0.04964	0.00886	0.23299	0.04067	0.03404	0.00154	0.04964	0.00886	0.23299	0.04067	0.03404	0.00154	178	279	213	33	216	10	-1.39%
B21T72-24	188	204	0.92	0.05039	0.01721	0.23495	0.07992	0.03381	0.00133	0.05039	0.01721	0.23495	0.07992	0.03381	0.00133	213	529	214	66	214	8	0.00%
B21T72-25	143	191	0.75	0.05027	0.00885	0.23346	0.0404	0.03368	0.00137	0.05027	0.00885	0.23346	0.0404	0.03368	0.00137	207	288	213	33	214	9	-0.47%
B21T72-26	77	124	0.62	0.05054	0.01403	0.22923	0.06297	0.03289	0.00157	0.05054	0.01403	0.22923	0.06297	0.03289	0.00157	220	420	210	52	209	10	0.48%
B21T72-27	265	283	0.94	0.04996	0.00662	0.22664	0.02919	0.0329	0.00129	0.04996	0.00662	0.22664	0.02919	0.0329	0.00129	193	216	207	24	209	8	-0.96%
B21T72-28	145	193	0.75	0.05065	0.01137	0.2392	0.0531	0.03425	0.0014	0.05065	0.01137	0.2392	0.0531	0.03425	0.0014	225	351	218	44	217	9	0.46%
B21T72-29	193	216	0.9	0.05016	0.00786	0.22838	0.03506	0.03302	0.0013	0.05016	0.00786	0.22838	0.03506	0.03302	0.0013	202	266	209	29	209	8	0.00%
B21T72-30	89	133	0.67	0.05014	0.00936	0.22704	0.04138	0.03283	0.00154	0.05014	0.00936	0.22704	0.04138	0.03283	0.00154	201	290	208	34	208	10	0.00%
B21T72-31	110	162	0.68	0.05033	0.0046	0.23122	0.02064	0.03332	0.0011	0.05033	0.0046	0.23122	0.02064	0.03332	0.0011	210	141	211	17	211	7	0.00%
B21T72-32	144	199	0.72	0.04994	0.00422	0.22835	0.01886	0.03317	0.00104	0.04994	0.00422	0.22835	0.01886	0.03317	0.00104	192	130	209	16	210	6	-0.48%
B21T72-33	77	179	0.43	0.05014	0.00505	0.2257	0.02223	0.03265	0.0011	0.05014	0.00505	0.2257	0.02223	0.03265	0.0011	201	159	207	18	207	7	0.00%
B21T72-34	172	212	0.81	0.05029	0.00452	0.22696	0.02001	0.03273	0.00102	0.05029	0.00452	0.22696	0.02001	0.03273	0.00102	208	142	208	17	208	6	0.00%
B21T72-35	99	152	0.65	0.05016	0.0077	0.22608	0.03437	0.03269	0.00112	0.05016	0.0077	0.22608	0.03437	0.03269	0.00112	202	269	207	28	207	7	0.00%
B21T72-36	183	222	0.82	0.05007	0.00924	0.23206	0.04267	0.03361	0.001	0.05007	0.00924	0.23206	0.04267	0.03361	0.001	198	318	212	35	213	6	-0.47%
B21T72-37	62	127	0.49	0.04991	0.00947	0.22565	0.0424	0.03279	0.00123	0.04991	0.00947	0.22565	0.0424	0.03279	0.00123	191	313	207	35	208	8	-0.48%
B21T72-38	129	185	0.7	0.05001	0.00909	0.22055	0.03988	0.03198	0.00101	0.05001	0.00909	0.22055	0.03988	0.03198	0.00101	195	308	202	33	203	6	-0.49%
B21T72-39	112	179	0.63	0.05035	0.00425	0.234	0.01935	0.03371	0.00104	0.05035	0.00425	0.234	0.01935	0.03371	0.00104	211	131	213	16	214	6	-0.47%
B21T72-40	100	151	0.66	0.05005	0.00579	0.22444	0.02547	0.03252	0.00113	0.05005	0.00579	0.22444	0.02547	0.03252	0.00113	197	191	206	21	206	7	0.00%
B21T73-01	116	174	0.67	0.05023	0.01316	0.22685	0.05925	0.03264	0.00114	0.05023	0.01316	0.22685	0.05925	0.03264	0.00114	206	415	208	49	207	7	0.48%
B21T73-02	264	278	0.95	0.04989	0.00823	0.22717	0.03732	0.03292	0.00102	0.04989	0.00823	0.22717	0.03732	0.03292	0.00102	190	283	208	31	209	6	-0.48%
B21T73-03	79	137	0.58	0.05015	0.02068	0.21731	0.08943	0.03133	0.00119	0.05015	0.02068	0.21731	0.08943	0.03133	0.00119	202	654	200	75	199	7	0.50%
B21T73-04	307	378	0.81	0.05517	0.00736	0.25563	0.03406	0.03351	0.00096	0.05517	0.00736	0.25563	0.03406	0.03351	0.00096	419	247	231	28	212	6	8.96%
B21T73-05	1284	829	1.55	0.05022	0.00438	0.23346	0.02045	0.03364	0.00087	0.05022	0.00438	0.23346	0.02045	0.03364	0.00087	205	150	213	17	213	5	0.00%
B21T73-06	356	393	0.91	0.05017	0.00712	0.22456	0.0318	0.03239	0.00093	0.05017	0.00712	0.22456	0.0318	0.03239	0.00093	203	259	206	26	205	6	0.49%
B21T73-07	693	666	1.04	0.0501	0.00433	0.22908	0.01985	0.03309	0.00088	0.0501	0.00433	0.22908	0.01985	0.03309	0.00088	200	146	209	16	210	5	-0.48%

B21T73-08	858	696	1.23	0.05045	0.00398	0.2331	0.01846	0.03345	0.00087	0.05045	0.00398	0.2331	0.01846	0.03345	0.00087	216	132	213	15	212	5	0.47%			
B21T73-09	99	137	0.73	0.05009	0.01066	0.22197	0.04692	0.03209	0.00118	0.05009	0.01066	0.22197	0.04692	0.03209	0.00118	199	339	204	39	204	7	0.00%			
B21T73-10	262	315	0.83	0.04926	0.00342	0.22091	0.01514	0.03248	0.00095	0.04926	0.00342	0.22091	0.01514	0.03248	0.00095	160	102	203	13	206	6	-1.46%			
B21T73-11	241	311	0.77	0.05023	0.00674	0.23684	0.03174	0.03416	0.00097	0.05023	0.00674	0.23684	0.03174	0.03416	0.00097	206	245	216	26	217	6	-0.46%			
B21T73-12	205	258	0.79	0.05035	0.00415	0.23457	0.01915	0.03375	0.00099	0.05035	0.00415	0.23457	0.01915	0.03375	0.00099	211	131	214	16	214	6	0.00%			
B21T73-13	237	214	1.11	0.04988	0.00725	0.21828	0.03147	0.03171	0.00103	0.04988	0.00725	0.21828	0.03147	0.03171	0.00103	189	257	200	26	201	6	-0.50%			
B21T73-14	844	602	1.4	0.05014	0.00248	0.23088	0.01115	0.03338	0.00087	0.05014	0.00248	0.23088	0.01115	0.03338	0.00087	201	68	211	9	212	5	-0.47%			
B21T73-15	238	288	0.83	0.05042	0.00386	0.22966	0.01743	0.03302	0.00095	0.05042	0.00386	0.22966	0.01743	0.03302	0.00095	214	120	210	14	209	6	0.48%			
B21T73-16	161	231	0.7	0.04977	0.0038	0.22161	0.01663	0.03229	0.00098	0.04977	0.0038	0.22161	0.01663	0.03229	0.00098	184	115	203	14	205	6	-0.98%			
B21T73-17	386	406	0.95	0.04995	0.00438	0.224	0.01962	0.03252	0.00089	0.04995	0.00438	0.224	0.01962	0.03252	0.00089	193	147	205	16	206	6	-0.49%			
B21T73-18	1920	1018	1.89	0.05054	0.00265	0.2267	0.01206	0.03253	0.00081	0.05054	0.00265	0.2267	0.01206	0.03253	0.00081	220	77	207	10	206	5	0.49%			
B21T73-19	113	168	0.67	0.05026	0.00773	0.22729	0.03465	0.03281	0.0011	0.05026	0.00773	0.22729	0.03465	0.03281	0.0011	207	271	208	29	208	7	0.00%			
B21T73-20	99	165	0.6	0.05042	0.00525	0.2303	0.02361	0.03314	0.00107	0.05042	0.00525	0.2303	0.02361	0.03314	0.00107	214	171	210	19	210	7	0.00%			
B21T73-21	249	329	0.76	0.04991	0.00298	0.23428	0.01388	0.03406	0.00094	0.04991	0.00298	0.23428	0.01388	0.03406	0.00094	191	86	214	11	216	6	-0.93%			
B21T73-22	360	416	0.87	0.05042	0.00267	0.22981	0.01203	0.03309	0.00091	0.05042	0.00267	0.22981	0.01203	0.03309	0.00091	214	71	210	10	210	6	0.00%			
B21T73-23	393	437	0.9	0.05028	0.0027	0.2293	0.01226	0.03311	0.00089	0.05028	0.0027	0.2293	0.01226	0.03311	0.00089	208	75	210	10	210	6	0.00%			
B21T73-24	251	359	0.7	0.04942	0.00315	0.22694	0.01419	0.03334	0.00097	0.04942	0.00315	0.22694	0.01419	0.03334	0.00097	168	91	208	12	211	6	-1.42%			
B21T73-25	522	542	0.96	0.05013	0.00306	0.21948	0.01328	0.03179	0.00086	0.05013	0.00306	0.21948	0.01328	0.03179	0.00086	201	90	201	11	202	5	-0.50%			
B21T73-26	543	647	0.84	0.05033	0.00294	0.22246	0.01288	0.0321	0.00087	0.05033	0.00294	0.22246	0.01288	0.0321	0.00087	210	84	204	11	204	5	0.00%			
B21T73-27	320	452	0.71	0.05013	0.00353	0.2245	0.01567	0.03253	0.0009	0.05013	0.00353	0.2245	0.01567	0.03253	0.0009	201	109	206	13	206	6	0.00%			
B21T73-28	133	183	0.73	0.04959	0.00892	0.223	0.03994	0.03266	0.00102	0.04959	0.00892	0.223	0.03994	0.03266	0.00102	176	305	204	33	207	6	-1.45%			
B21T73-29	336	464	0.72	0.05049	0.00282	0.23261	0.01295	0.03347	0.00088	0.05049	0.00282	0.23261	0.01295	0.03347	0.00088	218	81	212	11	212	5	0.00%			
B21T73-30	1179	1047	1.13	0.05149	0.00309	0.22075	0.01327	0.03115	0.0008	0.05149	0.00309	0.22075	0.01327	0.03115	0.0008	263	91	203	11	198	5	2.53%			
B21T73-31	28	77	0.37	0.05032	0.00619	0.22805	0.02622	0.03292	0.00169	0.05032	0.00619	0.22805	0.02622	0.03292	0.00169	210	165	209	22	209	11	0.00%			
B21T73-32	158	221	0.71	0.05011	0.0046	0.2355	0.02108	0.03408	0.00113	0.05011	0.0046	0.2355	0.02108	0.03408	0.00113	200	141	215	17	216	7	-0.46%			
B21T73-33	494	416	1.19	0.05001	0.00389	0.22443	0.01725	0.03254	0.00091	0.05001	0.00389	0.22443	0.01725	0.03254	0.00091	195	123	206	14	206	6	0.00%			

Detailed Data Analysis - Q3 2023																						
Category	Series ID	Geographic Metrics		Performance Indicators										Market & Economic								
		Region	Area	Revenue (M)	Profit (M)	Margin (%)	Units Sold	YTD Growth (%)	Unit Price (\$)	Cost (\$)	Margin (%)	Revenue (M)	Profit (M)	Margin (%)	Units Sold	YTD Growth (%)	Unit Price (\$)	Cost (\$)	Margin (%)	Revenue (M)	Profit (M)	Margin (%)
B21T73-34	527	540	0.98	0.05006	0.00259	0.23446	0.01203	0.03397	0.00088	0.05006	0.00259	0.23446	0.01203	0.03397	0.00088	198	72	214	10	215	5	-0.47%
B21T73-35	2152	1179	1.82	0.05052	0.00265	0.21852	0.01152	0.03136	0.00078	0.05052	0.00265	0.21852	0.01152	0.03136	0.00078	219	76	201	10	199	5	1.01%
B21T73-36	236	253	0.93	0.05017	0.00346	0.23247	0.01546	0.0336	0.00105	0.05017	0.00346	0.23247	0.01546	0.0336	0.00105	203	97	212	13	213	7	-0.47%
B21T73-37	267	327	0.82	0.05044	0.00455	0.22056	0.01971	0.03171	0.00089	0.05044	0.00455	0.22056	0.01971	0.03171	0.00089	215	150	202	16	201	6	0.50%
B21T73-38	473	384	1.23	0.04988	0.00549	0.22379	0.02448	0.03253	0.00092	0.04988	0.00549	0.22379	0.02448	0.03253	0.00092	189	193	205	20	206	6	-0.49%
B21T73-39	184	245	0.75	0.05003	0.00355	0.22192	0.01543	0.03216	0.00094	0.05003	0.00355	0.22192	0.01543	0.03216	0.00094	196	105	204	13	204	6	0.00%
B21T73-40	1664	992	1.68	0.05035	0.00218	0.23115	0.01002	0.03329	0.00083	0.05035	0.00218	0.23115	0.01002	0.03329	0.00083	211	56	211	8	211	5	0.00%
B21T73-41	172	313	0.55	0.04999	0.0048	0.23043	0.02195	0.03342	0.00093	0.04999	0.0048	0.23043	0.02195	0.03342	0.00093	195	163	211	18	212	6	-0.47%
B21T76-01	68	131	0.52	0.05019	0.00712	0.21635	0.03003	0.03128	0.00123	0.05019	0.00712	0.21635	0.03003	0.03128	0.00123	204	235	199	25	199	8	0.00%
B21T76-02	30	95	0.32	0.0503	0.01013	0.23021	0.04537	0.03321	0.00165	0.0503	0.01013	0.23021	0.04537	0.03321	0.00165	209	310	210	37	211	10	-0.47%
B21T76-03	256	260	0.99	0.05013	0.0065	0.22287	0.0287	0.03226	0.00097	0.05013	0.0065	0.22287	0.0287	0.03226	0.00097	201	234	204	24	205	6	-0.49%
B21T76-04	121	200	0.6	0.05017	0.00601	0.21675	0.0257	0.03135	0.00099	0.05017	0.00601	0.21675	0.0257	0.03135	0.00099	203	208	199	21	199	6	0.00%
B21T76-05	55	114	0.48	0.05004	0.01309	0.21374	0.05553	0.031	0.00127	0.05004	0.01309	0.21374	0.05553	0.031	0.00127	197	404	197	46	197	8	0.00%
B21T76-06	331	463	0.71	0.05037	0.00496	0.22045	0.02169	0.03175	0.00084	0.05037	0.00496	0.22045	0.02169	0.03175	0.00084	212	173	202	18	201	5	0.50%
B21T76-07	408	513	0.8	0.05041	0.00381	0.22306	0.01682	0.0321	0.00084	0.05041	0.00381	0.22306	0.01682	0.0321	0.00084	214	123	204	14	204	5	0.00%
B21T76-08	475	552	0.86	0.04973	0.00241	0.22311	0.01085	0.03255	0.00084	0.04973	0.00241	0.22311	0.01085	0.03255	0.00084	182	66	204	9	206	5	-0.97%
B21T76-09	80	233	0.34	0.0503	0.00467	0.22449	0.02065	0.03237	0.00094	0.0503	0.00467	0.22449	0.02065	0.03237	0.00094	209	153	206	17	205	6	0.49%
B21T76-10	828	815	+02	0.05337	0.00292	0.24064	0.01332	0.03271	0.00081	0.05337	0.00292	0.24064	0.01332	0.03271	0.00081	345	81	219	+11	207	5	5.80%
B21T76-11	53	112	0.48	0.05001	0.0068	0.21579	0.02876	0.0313	0.00121	0.05001	0.0068	0.21579	0.02876	0.0313	0.00121	195	228	198	24	199	8	-0.50%
B21T76-12	148	209	0.71	0.05022	0.00448	0.23069	0.02036	0.03332	0.00099	0.05022	0.00448	0.23069	0.02036	0.03332	0.00099	205	144	211	17	211	6	0.00%
B21T76-13	127	222	0.57	0.05022	0.0037	0.22467	0.01629	0.03244	0.00097	0.05022	0.0037	0.22467	0.01629	0.03244	0.00097	205	111	206	14	206	6	0.00%
B21T76-14	992	868	+14	0.05213	0.00282	0.2336	0.0128	0.0325	0.00081	0.05213	0.00282	0.2336	0.0128	0.0325	0.00081	291	80	213	+11	206	5	3.40%
B21T76-15	105	170	0.62	0.05014	0.00457	0.22459	0.02013	0.03248	0.00103	0.05014	0.00457	0.22459	0.02013	0.03248	0.00103	201	144	206	17	206	6	0.00%
B21T76-16	90	153	0.59	0.05089	0.00823	0.23203	0.03733	0.03306	0.00107	0.05089	0.00823	0.23203	0.03733	0.03306	0.00107	236	283	212	31	210	7	0.95%
B21T76-17	478	580	0.82	0.05161	0.00355	0.23185	0.01605	0.03257	0.00084	0.05161	0.00355	0.23185	0.01605	0.03257	0.00084	268	111	212	13	207	5	2.42%
B21T76-18	275	360	0.76	0.05154	0.00574	0.22796	0.02535	0.03207	0.00089	0.05154	0.00574	0.22796	0.02535	0.03207	0.00089	265	199	209	21	203	6	2.96%

B21T76-19	510	547	0.93	0.05002	0.00423	0.22873	0.01937	0.03315	0.00089	0.05002	0.00423	0.22873	0.01937	0.03315	0.00089	196	141	209	16	210	6	-0.48%
B21T76-20	198	223	0.89	0.05678	0.00401	0.26702	0.01858	0.03411	0.00103	0.05678	0.00401	0.26702	0.01858	0.03411	0.00103	483	101	240	15	216	6	11.11%
B21T76-21	448	479	0.94	0.05041	0.00353	0.23433	0.01645	0.0337	0.00091	0.05041	0.00353	0.23433	0.01645	0.0337	0.00091	214	111	214	14	214	6	0.00%
B21T76-22	192	234	0.82	0.04992	0.00804	0.23227	0.03726	0.03374	0.00106	0.04992	0.00804	0.23227	0.03726	0.03374	0.00106	191	277	212	31	214	7	-0.93%
B21T76-23	84	134	0.62	0.05022	0.0069	0.22603	0.03077	0.03263	0.00112	0.05022	0.0069	0.22603	0.03077	0.03263	0.00112	205	239	207	25	207	7	0.00%
B21T76-24	386	414	0.93	0.04996	0.00275	0.23282	0.01287	0.03378	0.00093	0.04996	0.00275	0.23282	0.01287	0.03378	0.00093	193	78	213	11	214	6	-0.47%
B21T76-25	398	506	0.79	0.04994	0.00251	0.23038	0.01169	0.03345	0.0009	0.04994	0.00251	0.23038	0.01169	0.03345	0.0009	192	69	211	10	212	6	-0.47%
B21T76-26	130	173	0.75	0.05028	0.00671	0.24114	0.03204	0.03477	0.00108	0.05028	0.00671	0.24114	0.03204	0.03477	0.00108	208	238	219	26	220	7	-0.45%
B21T76-27	465	446	1.04	0.05129	0.00443	0.24492	0.02124	0.03462	0.00094	0.05129	0.00443	0.24492	0.02124	0.03462	0.00094	254	147	222	17	219	6	1.37%
B21T76-28	157	241	0.65	0.05009	0.00452	0.22934	0.0203	0.03319	0.00111	0.05009	0.00452	0.22934	0.0203	0.03319	0.00111	199	138	210	17	210	7	0.00%
B21T76-29	556	763	0.73	0.05028	0.00211	0.22998	0.00965	0.03317	0.00083	0.05028	0.00211	0.22998	0.00965	0.03317	0.00083	208	53	210	8	210	5	0.00%
B21T76-30	175	238	0.74	0.0505	0.00923	0.22015	0.03998	0.03161	0.00102	0.0505	0.00923	0.22015	0.03998	0.03161	0.00102	218	309	202	33	201	6	0.50%
B21T76-31	487	452	1.08	0.05048	0.00287	0.22404	0.01247	0.03218	0.00089	0.05048	0.00287	0.22404	0.01247	0.03218	0.00089	217	78	205	10	204	6	0.49%
B21T76-32	288	304	0.95	0.0499	0.00338	0.23232	0.0155	0.03376	0.00094	0.0499	0.00338	0.23232	0.0155	0.03376	0.00094	190	102	212	13	214	6	-0.93%
B21T76-33	106	292	0.36	0.0502	0.00605	0.22527	0.02681	0.03253	0.00102	0.0502	0.00605	0.22527	0.02681	0.03253	0.00102	204	209	206	22	206	6	0.00%
B21T76-34	277	435	0.64	0.05014	0.0035	0.22912	0.0157	0.03313	0.00094	0.05014	0.0035	0.22912	0.0157	0.03313	0.00094	201	105	209	13	210	6	-0.48%
B21T76-35	1274	1096	1.16	0.0501	0.0028	0.22147	0.01236	0.03205	0.00079	0.0501	0.0028	0.22147	0.01236	0.03205	0.00079	200	84	203	10	203	5	0.00%
B21T76-36	320	437	0.73	0.05053	0.00449	0.2206	0.01946	0.03165	0.00086	0.05053	0.00449	0.2206	0.01946	0.03165	0.00086	219	149	202	16	201	5	0.50%
B21T76-37	294	225	1.31	0.0502	0.00411	0.22038	0.01754	0.03183	0.001	0.0502	0.00411	0.22038	0.01754	0.03183	0.001	204	123	202	15	202	6	0.00%

298

299

300

301

Table S9 Zircon LA-ICP-MS U-Pb data of the magmatic rocks in the Zhonggang intraplate ocean island fragment in the BNSZ

Spots	isotope ratio ($\pm 1\sigma$) (measured ratios)						isotope ratio ($\pm 1\sigma$) (corrected ratios)						age (Ma $\pm 1\sigma$)						
	$^{207}\text{Pb}/^{206}\text{Pb}$		$^{207}\text{Pb}/^{235}\text{U}$		$^{206}\text{Pb}/^{238}\text{U}$		$^{207}\text{Pb}/^{206}\text{Pb}$		$^{207}\text{Pb}/^{235}\text{U}$		$^{206}\text{Pb}/^{238}\text{U}$		$^{207}\text{Pb}/^{206}\text{Pb}$		$^{207}\text{Pb}/^{235}\text{U}$		$^{206}\text{Pb}/^{238}\text{U}$		Discordance
	ratios	1σ	ratios	1σ	ratios	1σ	ratios	1σ	ratios	1σ	ratios	1σ	age	ratio	age	1σ	age	1σ	
ZGT1-04	0.04953	0.00475	0.16247	0.01524	0.02375	0.00069	0.04953	0.00475	0.16247	0.01524	0.02375	0.00069	173	157	153	13	151	4	1.32%
ZGT1-08	0.04826	0.00164	0.15203	0.00506	0.02281	0.00048	0.04826	0.00164	0.15203	0.00506	0.02281	0.00048	112	41	144	4	145	3	-0.69%
ZGT1-11	0.04783	0.01226	0.14353	0.03665	0.02175	0.00066	0.04783	0.01226	0.14353	0.03665	0.02175	0.00066	91	395	136	33	139	4	-2.16%
ZGT1-01	0.0508	0.00966	0.16324	0.03089	0.0233	0.00075	0.0508	0.00966	0.16324	0.03089	0.0233	0.00075	232	325	154	27	148	5	4.05%
ZGT1-02	0.04952	0.01235	0.15398	0.03824	0.02255	0.0008	0.04952	0.01235	0.15398	0.03824	0.02255	0.0008	173	390	145	34	144	5	0.69%
ZGT1-04	0.05196	0.00712	0.15419	0.02095	0.02152	0.00069	0.05196	0.00712	0.15419	0.02095	0.02152	0.00069	284	247	146	18	137	4	6.57%
ZGT2-01	0.04732	0.00891	0.14418	0.02699	0.02209	0.00066	0.04732	0.00891	0.14418	0.02699	0.02209	0.00066	65	294	137	24	141	4	-2.84%
ZGT2-02	0.05023	0.0057	0.15318	0.01713	0.0221	0.00063	0.05023	0.0057	0.15318	0.01713	0.0221	0.00063	206	198	145	15	141	4	2.84%
ZGT2-03	0.04626	0.00856	0.14391	0.02647	0.02255	0.00067	0.04626	0.00856	0.14391	0.02647	0.02255	0.00067	11	286	137	23	144	4	-4.86%
ZGT2-07	0.04748	0.00468	0.14249	0.01393	0.02175	0.00055	0.04748	0.00468	0.14249	0.01393	0.02175	0.00055	73	169	135	12	139	3	-2.88%
ZGT2-08	0.05093	0.00636	0.14495	0.01775	0.02063	0.00069	0.05093	0.00636	0.14495	0.01775	0.02063	0.00069	238	214	137	16	132	4	3.79%
ZGT2-02	0.04857	0.0057	0.14288	0.01669	0.02133	0.0006	0.04857	0.0057	0.14288	0.01669	0.02133	0.0006	127	209	136	15	136	4	0.00%
ZGT2-03	0.04805	0.00377	0.14681	0.01147	0.02216	0.00058	0.04805	0.00377	0.14681	0.01147	0.02216	0.00058	102	125	139	10	141	4	-1.42%
ZGT3-07	0.04974	0.0059	0.15541	0.01816	0.02266	0.00073	0.04974	0.0059	0.15541	0.01816	0.02266	0.00073	183	203	147	16	144	5	2.08%
ZGT3-08	0.04917	0.00722	0.15098	0.02204	0.02227	0.00066	0.04917	0.00722	0.15098	0.02204	0.02227	0.00066	156	254	143	19	142	4	0.70%
ZGT3-09	0.04871	0.0046	0.1573	0.01454	0.02342	0.00074	0.04871	0.0046	0.1573	0.01454	0.02342	0.00074	134	148	148	13	149	5	-0.67%
ZGT3-07	0.05069	0.01241	0.14602	0.03563	0.02089	0.00071	0.05069	0.01241	0.14602	0.03563	0.02089	0.00071	227	395	138	32	133	4	3.76%
ZGT3-10	0.05078	0.00604	0.15864	0.01876	0.02266	0.00065	0.05078	0.00604	0.15864	0.01876	0.02266	0.00065	231	213	150	16	144	4	4.17%
ZGT3-14	0.04628	0.00667	0.14702	0.02112	0.02304	0.00065	0.04628	0.00667	0.14702	0.02112	0.02304	0.00065	12	236	139	19	147	4	-5.44%

304

Table S10 Sphene LA–ICP–MS U–Pb data of the magmatic rocks in the Zhonggang intraplate ocean island fragment in the BNSZ

Spots	Th	U	207Pb/206Pb ratios	207Pb/206Pb 1σ	207Pb/235U ratios	207Pb/235U 1σ	206Pb/238U ratios	206Pb/238U 1σ	207Pb/206Pb Age (Ma)	207Pb/206Pb 1σ	207Pb/235U Age (Ma)	207Pb/235U 1σ	206Pb/238U Age (Ma)	206Pb/238U 1σ
B22T14-01	0.11	14.0	0.5930	0.0372	12.1795	1.1088	0.1479	0.0098	4491	91.33	2618	85.4	889	54.8
B22T14-02	112	24.9	0.3258	0.0299	2.1870	0.1911	0.0522	0.0027	3597	141.4	1177	60.9	328	16.8
B22T14-03	0.022	10.3	0.2908	0.0734	1.5140	0.1724	0.0310	0.0028	3422	403	936	69.6	197	17.3
B22T14-04	0.066	11.1	0.2298	0.0443	1.0100	0.0810	0.0284	0.0017	3050	314	709	40.9	180	10.9
B22T14-05	0.042	27.4	0.2728	0.0277	1.2409	0.0903	0.0325	0.0013	3322	160	819	40.9	206	8.2
B22T14-06	0.076	11.1	0.3060	0.0730	1.7939	0.2371	0.0338	0.0030	3501	378	1043	86.2	214	18.6
B22T14-07	0.66	12.9	0.1961	0.0266	1.2660	0.1145	0.0340	0.0017	2794	223	831	51.3	216	10.5
B22T14-08	112	24.2	0.2999	0.0267	1.6649	0.1152	0.0441	0.0014	3469	138	995	43.9	278	8.6
B22T14-09	0.10	5.35	0.3179	0.0582	3.9147	0.4486	0.0507	0.0032	3560	285	1617	92.7	319	19.4
B22T14-10	0.049	5.16	0.3130	0.0529	3.1597	0.3018	0.0427	0.0027	3536	264	1447	73.7	269	16.5
B22T14-11	0.063	5.63	0.4312	0.0657	4.8938	0.5333	0.0469	0.0040	4022	230	1801	91.9	296	24.6
B22T14-12	0.092	8.93	0.4314	0.0559	3.1940	0.2278	0.0659	0.0032	4033	195	1456	55.2	412	19.5

305

306

307

308

309

Table S11 Bulk-rock Sr–Nd isotopic composition of the magmatic rocks in the intraplate ocean island fragments in the BNSZ

		Sample	Lithology	Reference	Age (Ma)	Rb	Sr	$^{87}\text{Sr}/^{86}\text{Sr}$	2σ	$^{87}\text{Rb}/^{86}\text{Sr}$	$(^{87}\text{Sr}/^{86}\text{Sr})\text{i}$	Sm	Nd	$^{143}\text{Nd}/^{144}\text{Nd}$	2σ	$^{147}\text{Sm}/^{144}\text{Nd}$	$(^{143}\text{Nd}/^{144}\text{Nd})\text{i}$	$\epsilon_{\text{Nd}}(\text{t})$
Nare ocean island fragment	CT13T1H2	Trachyte	This study	245	135.72	27.46	0.705599	0.000007	44.29771336	0.656788902	17.91	94.14	0.512828	0.000006	0.114605626	0.512648081	6.23	
	Z15T1H1	Trachyte	This study	245	46.42	27.74	0.706104	0.000008	4.83997802	0.689581468	12.43	69.74	0.512820	0.000005	0.107365107	0.512651204	6.29	
	Z15T1H4	Trachyte	This study	245	86.79	21.30	0.741778	0.000009	11.83106277	0.701389221	14.60	76.44	0.512695	0.000005	0.115064777	0.512513775	3.61	
	B21T61h5	Trachyte	This study	245	143.8	31.61	0.736773	0.000008	13.20019607	0.69076936	16.72	85.86	0.512718	0.000004	0.117305568	0.512529974	4.05	
	B21T61h6	Trachyte	This study	245	400.3	29.15	0.729015	0.000007	9.976531666	0.694246398	15.95	82.33	0.512713	0.000005	0.11670119	0.512525845	3.97	
	B21T61h8	Trachyte	This study	245	75.39	24.41	0.728514	0.000007	8.954512049	0.697306997	17.06	90.71	0.512715	0.000004	0.113291352	0.512533113	4.11	
Maqiao ocean island fragment	ShT42H1	Trachyte	This study	205	22.71	174.70	0.705220	0.000007	0.376038	0.704124	11.69	57.42	0.512719	0.000006	0.122637889	0.512554576	3.52	
	B19T27H2	Trachyandesite	This study	205	19.85	429.24	0.705299	0.000007	0.133785	0.704909	14.21	72.32	0.512732	0.000005	0.118319973	0.512573019	3.88	
	B19T30H2	Phonolite	This study	205	29.76	182.34	0.707062	0.000007	0.472174	0.705686	21.03	141.86	0.512765	0.000006	0.089285945	0.512645712	5.30	
	B21T28h4	Basalt	This study	205	3.041	658.9	0.703741	0.000008	0.013349	0.703702	5.043	19.86	0.512902	0.000004	0.152968454	0.512696887	6.30	
	B21T28h5	Basalt	This study	205	3.707	364.2	0.703854	0.000007	0.029440	0.703768	5.235	20.45	0.512908	0.000004	0.154211281	0.512701249	6.38	
	B21T28h6	Basalt	This study	205	2.189	601.2	0.703765	0.000009	0.010531	0.703734	5.256	21.05	0.512915	0.000005	0.150416947	0.51271356	6.63	
Tarenben ocean island fragment	B21T68h1	Basalt	This study	209	11.41	373.3	0.705286	0.000006	0.088417	0.705023	3.335	12.68	0.512893	0.000004	0.158441096	0.512676656	6.01	
	B21T69h1	Basalt	This study	209	9.114	439.1	0.705163	0.000006	0.060041	0.704985	3.975	15.65	0.512803	0.000004	0.1530047	0.51259386	4.39	
	B21T70h2	Basalt	This study	209	3.868	300.2	0.704880	0.000005	0.037271	0.704770	3.768	14.03	0.512879	0.000004	0.161786754	0.512657329	5.63	
	B21T72h2	Trachyte	This study	209	1.385	197.8	0.704919	0.000008	0.020254	0.704859	13.46	77.81	0.512803	0.000004	0.104205731	0.512660412	5.69	
	B21T73h1	Trachyandesite	This study	209	1.963	487.2	0.704161	0.000007	0.011654	0.704127	12.92	64.66	0.512820	0.000004	0.12036787	0.512655831	5.60	
	B21T76h2	Basalt	This study	209	50.27	1160	0.704549	0.000007	0.125352	0.704177	12.74	62.73	0.512811	0.000004	0.122342381	0.51264367	5.36	
Gufeng ocean island fragment	B21T77h2	Basalt	This study	209	34.45	373.2	0.705372	0.000008	0.267031	0.704579	11.48	59.25	0.512800	0.000004	0.116717278	0.512639974	5.29	
	DT13T6h8	Trachyandesite	This study	215	13.136	324.6	0.707498	0.000006	0.117090	0.707140	6.064	26.94	0.512838	0.000005	0.135596094	0.512647351	5.58	
	DT13T6h9	Trachyandesite	This study	215	21.98	310	0.707572	0.000006	0.205151	0.706945	6.962	32.04	0.512839	0.000004	0.130896227	0.512654334	5.72	
	DT13T6h10	Trachyandesite	This study	215	15.864	350.6	0.707425	0.000007	0.130919	0.707025	6.956	32.36	0.512834	0.000003	0.129489998	0.512651913	5.67	

Zhonggang ocean island fragment	D18T22	Trachyandesite	Fan et al., 2021	140	1.50	299	0.704043	0.000038	0.0145	0.704014	18.0	78.8	0.512813	0.000005	0.1377	0.512686	4.46
	Oz4H2	basalt	Fan et al., 2021	140	22.2	480	0.705694	0.000003	0.1336	0.705428	8.58	38.0	0.512781	0.000005	0.1359	0.512657	3.88
	Oz2H1	basalt	Fan et al., 2021	140	9.69	255	0.705568	0.000004	0.1098	0.705349	5.27	21.0	0.512796	0.000005	0.1511	0.512658	3.91
	DC13T1H3	basalt	Fan et al., 2021	140	38.3	1279	0.704459	0.000004	0.0865	0.704286	10.1	45.2	0.512804	0.000004	0.1347	0.512681	4.35
	DC13T1H9	Trachyandesite	Fan et al., 2021	140	37	490	0.704803	0.000003	0.2186	0.704367	15.1	73.5	0.512810	0.000005	0.1241	0.512697	4.66
	DC13T1H14	basalt	Fan et al., 2021	140	9.95	271	0.704472	0.000004	0.1063	0.704260	8.99	44.4	0.512828	0.000005	0.1219	0.512716	5.04
	11 DC-25	basalt	Wang et al., 2016	140	61.4	355	0.705266	0.000004	0.5003	0.704270	8.04	39.2	0.512825	0.000005	0.1236	0.512712	4.96
	11 DC-26	basalt	Wang et al., 2016	140	10.2	403	0.704246	0.000005	0.0732	0.704100	8.03	39.7	0.512831	0.000006	0.1218	0.512719	5.10
	11 DC-27	basalt	Wang et al., 2016	140	29.4	571	0.704604	0.000004	0.1489	0.704308	8.43	41.4	0.512805	0.000005	0.1227	0.512693	4.58
	11 DC-28	basalt	Wang et al., 2016	140	57.6	417	0.705626	0.000004	0.3996	0.704831	11.6	62.4	0.512830	0.000006	0.1120	0.512727	5.26
	11 DC-30	basalt	Wang et al., 2016	140	1.26	221	0.704025	0.000005	0.0165	0.703992	8.69	41.2	0.512875	0.000007	0.1271	0.512759	5.87
	11 DC-40	basalt	Wang et al., 2016	140	44.5	81.5	0.707281	0.000004	1.5798	0.704137	4.98	20.8	0.512897	0.000008	0.1442	0.512765	5.99
	11 DC-41	basalt	Wang et al., 2016	140	23.1	181	0.705409	0.000004	0.3692	0.704674	6.99	29.7	0.512861	0.000005	0.1418	0.512731	5.33
	11 DC-42	basalt	Wang et al., 2016	140	15.6	155	0.705058	0.000003	0.2911	0.704479	6.85	29.7	0.512854	0.000005	0.1389	0.512727	5.25
	11 DC-43	basalt	Wang et al., 2016	140	39.4	258	0.705618	0.000004	0.4418	0.704739	7.98	34.5	0.512851	0.000004	0.1393	0.512723	5.18
	11 DC-44	basalt	Wang et al., 2016	140	14.2	154	0.705062	0.000004	0.2667	0.704531	6.75	28.2	0.512866	0.000005	0.1442	0.512734	5.39